Adaptation by Loss of Heterozygosity in *Saccharomyces cerevisiae* Clones Under Divergent Selection

Timothy Y. James,*,[1] Lucas A. Michelotti,*,[2] Alexander D. Glasco,* Rebecca A. Clemons,* Robert A. Powers,* Ellen S. James,* D. Rabern Simmons,* Fengyan Bai,[†] and Shuhua Ge[‡]

*Department of Ecology and Evolutionary Biology, University of Michigan, Ann Arbor, Michigan 48109, [†]Institute of Microbiology, Chinese Academy of Sciences, State Key Laboratory of Mycology, Chaoyang District, Beijing 100101, China, and [‡]Technology Development and Transfer Center, Institute of Microbiology, Chinese Academy of Sciences, Chaoyang District, Beijing 100029, China

ORCID IDs: 0000-0002-1123-5986 (T.Y.J.); 0000-0002-5429-4548 (R.A.P.)

ABSTRACT Loss of heterozygosity (LOH) is observed during vegetative growth and reproduction of diploid genotypes through mitotic crossovers, aneuploidy caused by nondisjunction, and gene conversion. We aimed to test the role that LOH plays during adaptation of two highly heterozygous *Saccharomyces cerevisiae* genotypes to multiple environments over a short time span in the laboratory. We hypothesized that adaptation would be observed through parallel LOH events across replicate populations. Using genome resequencing of 70 clones, we found that LOH was widespread with 5.2 LOH events per clone after ~500 generations. The most common mode of LOH was gene conversion (51%) followed by crossing over consistent with either break-induced replication or double Holliday junction resolution. There was no evidence that LOH involved nondisjunction of whole chromosomes. We observed parallel LOH in both an environment-specific and environment-independent manner. LOH largely involved recombining existing variation between the parental genotypes, but also was observed after *de novo*, presumably beneficial, mutations occurred in the presence of canavanine, a toxic analog of arginine. One highly parallel LOH event involved the *ENA* salt efflux pump locus on chromosome IV, which showed repeated LOH to the allele from the European parent, an allele originally derived by introgression from *S. paradoxus*. Using CRISPR-engineered LOH we showed that the fitness advantage provided by this single LOH event was 27%. Overall, we found extensive evidence that LOH could be adaptive and is likely to be a greater source of initial variation than *de novo* mutation for rapid evolution of diploid genotypes.

KEYWORDS mitotic recombination; gene conversion; experimental evolution; *Saccharomyces cerevisiae*; resequencing

MITOTIC recombination is an unavoidable byproduct of the DNA repair process during growth or reproduction of diploid genotypes. Mitotic recombination may lead to a loss of heterozygosity (LOH) through a number of molecular mechanisms, such as gene conversion, crossing over, or DNA synthesis repair triggered by double-strand breaks (St Charles *et al.* 2012; Symington *et al.* 2014). In multicellular organisms, the end result of LOH is somatic variation, but in unicellular, asexual organisms, the effects of mitotic recombination manifest at the population level. Empirical studies show that genotypes that have undergone clear and recent LOH are common in populations of clonal or partially clonal diploids (Goodwin *et al.* 1994; Omilian *et al.* 2006; James *et al.* 2009; Magwene *et al.* 2011; Inbar *et al.* 2013; Hirakawa *et al.* 2015; Peter *et al.* 2018). It is an open question whether LOH in nature is a product of adaptive genotype change or instead reflects generally neutral or deleterious processes. Because LOH is associated with DNA damage and cancer progression through exposure of recessive mutations (Ryland *et al.* 2015), it has been largely been overlooked as an adaptive source of genotypic change, and efforts to understand its

doi: https://doi.org/10.1534/genetics.119.302411
Manuscript received June 7, 2019; accepted for publication July 29, 2019; published Early Online August 1, 2019.
Supplemental material available at FigShare: https://doi.org/10.25386/genetics.9118316.
[1]Corresponding author: University of Michigan, 1105 N. University, 4050 Biological Sciences Bldg., Ann Arbor, MI 48109. E-mail: tyjames@umich.edu
[2]Present address: Department of Entomology, University of Georgia, Athens, GA 30606.

role in adaptation of microbial eukaryotes are only beginning (Gerstein *et al.* 2014; Wertheimer *et al.* 2016; Smukowski Heil *et al.* 2017).

The most obvious context in which LOH could be adaptive is through exposure of a recessive beneficial allele previously masked in the heterozygous state. In this manner, mitotic recombination is predicted to allow asexual genotypes to adapt equally fast as sexual, because LOH occurs at a much higher rate than mutation, depending on genomic location (Mandegar and Otto 2007). Experimentally, this has been demonstrated in the evolution of *Saccharomyces cerevisiae* to the antifungal drug nystatin through LOH-mediated emergence of recessive resistance mutants in laboratory populations (Gerstein *et al.* 2014) or in hybrid yeast evolving to nutrient-limiting conditions (Smukowski Heil *et al.* 2017). Another important contribution of LOH to genotype evolution is through its potential to alleviate negative epistasis between alleles at heterozygous loci, such as observed in Dobzhansky–Muller incompatibilities between divergent genotypes (Johnson 2000; Wu and Ting 2004). The pervasiveness of both recessive beneficial mutations and negative epistasis across lifeforms (Zeyl *et al.* 2003; Hall and Joseph 2010; Orr 2010; Kvitek and Sherlock 2011) suggests that for organisms in which asexual reproduction dominates the life cycle, mitotic recombination might be as important for rapid adaptation as mutation.

Genotypes that show genome-wide heterozygosity may possess an abundant source of genetic variation that could be utilized for rapid evolution. Not only does LOH occur at a faster rate than mutation on a per nucleotide level (Omilian *et al.* 2006; Mandegar and Otto 2007; Wertheimer *et al.* 2016), but it also leverages natural genetic variation, which has been shown to be the favored variation for rapid evolution in experimentally evolved populations (Parts *et al.* 2011; Burke *et al.* 2014). In a typical laboratory evolution experiment, starting from genotypically homogeneous material, evolved strains acquire only a handful of mutations (Gresham *et al.* 2008; Conrad *et al.* 2009; Lang *et al.* 2013). This number is considerably lower than the amount of genotypic change that could occur due to LOH. On the other hand, LOH is completely reliant on the existence of heterozygous allelic variation for fitness in the environment in question. In the case of predictable evolution, such as resistance to antibiotics or toxins, resistance alleles for a given selective agent may not segregate in natural populations, presumably due to a high fitness tradeoff for resistance (Rosenthal 2013; Hill *et al.* 2015; Basra *et al.* 2018). LOH, nevertheless, plays a fundamental role in the evolution of asexual populations to these strong selective pressures through generating homozygous variants of recessive or partially recessive mutations that arise *de novo* (Cowen *et al.* 2000; Coste *et al.* 2006; Schoustra *et al.* 2007; Vázquez-Garcia *et al.* 2017).

The yeast species *S. cerevisiae* is a model for understanding the mechanism of mitotic recombination (Symington *et al.* 2014; Hum and Jinks-Robertson 2018). The signature of LOH in *S. cerevisiae* is strong in natural isolates; genome resequencing of diverse strains reveals LOH in essentially all strains (Magwene *et al.* 2011; Clowers *et al.* 2015; Peter *et al.* 2018). Whole-genome sequencing has been used to reveal the frequency of types of LOH events in yeast, but generally it is unclear the precise fitness effects that are associated with them (Dutta *et al.* 2017; Zhang *et al.* 2019), but see Gerstein *et al.* (2014), Smukowski Heil *et al.* (2017). Through its multiple mechanisms, LOH typically changes suites of linked nucleotides simultaneously (Symington *et al.* 2014). At its extreme, it can involve entire chromosomes. LOH of large numbers of linked sites should limit the benefit of LOH due to epistasis among the sites subjected to LOH. Because LOH also reduces the allelic diversity of a genotype, large LOH events also reduce the potential for further adaptation of genotypes by mitotic recombination, which may make LOH a form of short-sighted evolution. In cases where very strong selection imposed through exposure to drug or host pressure favors LOH, the resulting genotypes may not be well adapted to alternative environments and may lose generalist traits relative to their heterozygous progenitors, although this has yet to be demonstrated (Bennett *et al.* 2014). Thus, evidence indicates LOH facilitates evolution in the laboratory, but whether in more natural environments the observed LOH is the product of adaptive evolution or more neutral processes is unresolved.

Here, we test whether the heterozygosity in randomly outcrossed *S. cerevisiae* individuals contains fitness variation for diverse, natural environments that can be easily accessed by LOH during clonal evolution. Two ancestral, highly heterozygous genotypes were used to initiate the experiment; the high heterozygosity line (HHL) had $\sim 2\times$ the heterozygosity of the low heterozygosity line (LHL). We sequenced clones following 100 days of evolution, characterized their fitness, and estimated LOH and *de novo* mutation in clones using genome resequencing. Populations were kept at high effective sizes minimizing the effect of genetic drift and facilitating natural selection. We specifically tested for parallel LOH events across replicate populations of the same environment. We also examined whether the mechanism and rate of recombination would differ depending on initial heterozygosity and whether initial heterozygosity influenced gain in fitness over the experiment.

Materials and Methods

Strains and construction of ancestral genotypes

Strains were routinely propagated on standard yeast extract peptone dextrose (YPD; Difco) and stored at -80° in 25% glycerol. Haploid strains were modified to be *ho*Δ by integrating drug cassettes at the *HO* locus using standard methods (Maclean *et al.* 2017). We constructed two diploid ancestor strains of different initial heterozygosity by crossing two different haploid strains to a common genetic background (Table 1). The common genetic background was derived from

322134S, a clinical strain that shows distinct properties such as metabolite production and adhesion (MacKenzie *et al.* 2008; Hope and Dunham 2014), and has high pathogenic potential when tested in the insect larva *Galleria mellonella* (Phadke *et al.* 2018). The high heterozygosity genotype (SSP309, or HHL) was made by crossing SSP253 (*MAT*α derivative of 322134S) to SSP24 (*MATa* HN6 derivative) a Chinese strain from a basal *S. cerevisiae* lineage (Wang *et al.* 2012). The lower heterozygosity genotype (SSP272, or LHL) was made by crossing SSP245 (*MAT*α derivative of 322134S) to SSP264 (*MATa* YPS128 derivative), an oak isolate from Pennsylvania, with high fitness in rich media (Maclean *et al.* 2017). SSP272 was mated by plating together strains on YPD with drugs to select for diploids with complementary resistance markers, and SSP309 was mated on YPD without drugs and a diploid mating product identified by a PCR analysis of the *MAT* locus (Huxley *et al.* 1990). For the development of a competitor strain isogenic to SSP309 for estimates of relative fitness, the strain SSP330 was constructed by inserting a gene encoding red fluorescent protein (RFP) near the *MATa* locus as previously described (Chin *et al.* 2012), or through insertion of a YFP fluorescent marker driven by a *TDH3* promoter (gift from Patricia Wittkopp laboratory) to make strains LM3 and LM4.

Experimental passaging in vitro

We used the two ancestral genotypes to create independently evolving populations for 100 days of serial transfer. Each strain was grown in five media types; each type represented by eight replicate populations of 500 μl. The strains were grown in flat-bottom, autoclavable, deep-well (2 ml) plastic plates, with a separate plate for each strain and with populations ordered into a checkerboard pattern to reduce cross-contamination between wells.

The five media types used were YPD, beer wort, wine must, high salt, and minimal medium plus canavanine. Media compositions were experimentally adjusted so that all media types could be propagated using the same growth and transfer volumes. Beer wort comprised (per liter) 13% malt extract (Muntons Plain Light), 6 g Cascade hop flowers (Hopunion) boiled for 20 min, filtered through cheesecloth, and centrifuged for 10 min at 8000 rpm to remove debris. Wine must comprised (per liter) 250 ml red grape concentrate (Global Vintners). High salt comprised YPD with 1.0 M NaCl. Canavanine comprised of (per liter) 1.7 g yeast nitrogen base without amino acids and ammonium sulfate, 5 g $(NH_4)_2SO_4$, 20 g dextrose, 1.3 g yeast dropout powder minus arginine, 4 mg arginine, and 2 mg canavanine. All media was sterilized by autoclaving at 121° for 30 min.

To initiate the experiment the two heterozygous ancestors were grown overnight in 5 ml of YPD and 10 μl used to inoculate sterile media. The remaining culture was used for DNA extraction to serve as the reference ancestral genotypes for genome resequencing. Each day, at approximately the same time, we transferred 10 μl of the previous day's culture into 490 μl of fresh media. This dilution rate (1:50) was used to ensure that all populations could be transferred with the same frequency and volume, and implies a maximum of six generations per day when cultures reach saturation. Plates were incubated at 30° with shaking at 200 rpm. Every fifth passage, 25 μl of each population was subsampled for archiving in 25% glycerol at −80°. At the end of 100 days, one clone was isolated from each population by streak plating, and the remaining population archived.

Passaging by serial infection of G. mellonella

The hybrid ancestor SSP309 was serially passaged by injection into the last instar of the larvae of waxmoth, *G. mellonella*, as described previously (Phadke *et al.* 2018). Inoculum to initiate eight independent populations was generated by overnight growth at 30° in 10 ml liquid YPD medium. The density of the overnight culture was measured using a hemocytometer and adjusted to 10^9 cells/ml using sterile water. Each population contained five larvae injected through the last proleg with 10 μl of the initial inoculum, *i.e.*, at the density of 10^7 cells per larva. Larvae were housed at room temperature (20–22°) with ambient lighting. After 48 hr, yeast cells in each population were collected by crushing the five larvae together in a mortar and pestle and resuspending the extract in 20 ml sterile water after filtration through a sterile nylon filter (40 μm) to separate the yeast cells from the larval tissue. To obtain enough cells to inject a new batch of larvae for the next passage, 1–5 ml of the filtered extract was mixed with an equal volume of YPD containing G418 (200 μg/ml), ampicillin (1 mg/ml), and chloramphenicol (17 mg/ml) and grown overnight at 30° with shaking at 200 rpm. Following overnight growth, cells were pelleted, washed once with H_2O, and the density adjusted to 10^9 cells/ml using sterile water.

After the eighth passage in this manner, we observed the accumulation of insoluble black material in our homogenates (presumably melanin), which interfered with overnight growth and obtaining enough cells for reinfection. We then switched to a strategy in which 2 ml of the homogenate of each population was plated onto large (15 cm diameter) petri dishes containing YPD agar with the above mentioned drugs. This allowed cells to be isolated from the black material and robust overnight growth into lawns of over 10^4 colony-forming units per plate. After overnight growth, the cells were collected in 20 ml sterile water using cell scrapers, pelleted, washed with sterile water, and densities again adjusted to 10^9/ml prior to injecting for the next passage. After 12 additional passages of this strategy (20 total passages), individual clones from the populations were isolated by streak plating the homogenates. Stocks of the initial inoculum, passages, and isolated clones were made in 20% glycerol and stored at −80°.

Estimation of fitness

We estimated fitness of our evolved strains using both growth curves and competition with a reference strain. Growth curves were estimated using a Bioscreen C (Growth Curves USA) or a

Table 1 List of strains

Strain	Genotype	Background	Reference
LM3	*MATa/MATα ho::NAT/ho::pTDH3-YFP-KanMX4*	Cross of SSP245 × PJW1018	This study
LM4	*MATa/MATα ho::HYG/ ho::pTDH3-YFP-KanMX4*	Cross of SSP23 × PJW1029	This study
SSP23	*MATα ho::HYG*	HN6	Wang *et al.* (2012)
SSP24	*MATa ho::KanMX4*	HN6	Wang *et al.* (2012)
SSP245	*MATα ho::NAT*	322134S	MacKenzie *et al.* (2008)
SSP253	*MATα ho::KanMX4*	322134S	MacKenzie *et al.* (2008)
SSP264	*MATa-fasterMT-RFP-HYG ho::KanMX4*	YPS128	Sniegowski *et al.* (2002)
PJW1018	*MATa ho::pTDH3-YFP-KanMX4*	YPS128	P. J. Wittkopp laboratory
PJW1029	*MATa ho::pTDH3-YFP-KanMX4*	322134S	P. J. Wittkopp laboratory
SSP272	*MATa-fasterMT-RFP-HYG/MATα ho::NAT/ ho::KanMX4*	Cross of SSP245 × SSP264	Phadke *et al.* (2018)
SSP309	*MATa/MATα ho::KanMX4/ ho::KanMX4*	Cross of SSP24 × SSP253	This study
SSP330	*MATa-fasterMT-RFP-HYG/MATα ho::KanMX4/ ho::KanMX4*	Cross of SSP24 × SSP253	This study

Background indicates wild-type strain designation during original isolation or construction details as listed under the reference.

Synergy H1 (Biotek) plate spectrophotometer. Inoculum of evolved and ancestral strains was grown overnight in YPD at 30° by inoculating 500 μl of media directly from frozen stocks. Then, strains were diluted 100 fold and inoculated into the test media in a final volume of 200 μl. Each strain was run in eight replicates, and the ancestral strain was run on every plate. Growth curves were generated with incubation at 30° and readings of OD 600 taken every 20 min. Analysis of growth curves including correction for non-linearity between optical density and cell density were according to Warringer and Blomberg (2003).

Estimating fitness by competition to a common reference strain was also used as this known to produce different results than growth curves and may explain evolution among closely related genotypes more accurately (Wiser and Lenski 2015). Competition was measured by comparing proportions of unlabeled cells (evolved) with a near isogenic competitor strain designed to express YFP. The strain LM3 was used for strains evolved in the SSP272 background, and the strain LM4 was used for SSP309 evolution (Table 1). Strains were grown overnight from stocks in 500 μl of YPD and added in equal volumes (21.5 μl each) to a final volume of 550 μl test media. An aliquot of the cells was taken to measure the initial frequency of genotypes and compared with aliquots of the competing strains taken 24 hr later after growth at 30°. Cells were run undiluted or diluted at 1:3 or 1:10 (beer wort and wine must media only, respectively) into sterile PBS and analyzed on an iQue Screener PLUS (Intellicyt) with 5 sec sip time. Counts of yellow fluorescent events to nonfluorescent events were used to measure the cell ratios of reference to evolved strains. Approximately 2–10 × 10^4 cells were counted for each sample.

Fitness of Galleria passaged lines

We constructed the strain SSP330 to be near-isogenic with SSP309 but labeled with RFP to be used as a reference competitor strain for estimating virulence of the evolved lines post passaging in waxworms. Colonies of the RFP strain were found to be a distinct pale pink color after a few days incubation at 4°. We ultimately found that rather than using flow cytometry that counts of pink to white colonies was adequate to distinguish the two genotypes.

To estimate the relative fitness of the evolved lines we co-injected them into five larvae of *G. mellonella* as described above. To estimate initial genotype ratios, the mixed inoculum was plated before injection. Larvae were crushed in sterile water 48 hr postinjection and plated. Pre- and postinjection samples were plated on YPD media containing G418 and chloramphenicol and placed at 4° after 1 day incubation at 30°. We compared the relative fitness of the ancestor (SSP309) and competitor (SSP330) using three replicates in the above manner and detected no significant difference.

DNA manipulations and sequencing

Genome resequencing: We sequenced single clones from 46 *in vitro* populations, 24 clones from the eight *in vivo* populations (10 from population 1 and two from the other seven populations), the four parental haploid strains, and the two diploid ancestral strains (Supplemental Material, Table S1). DNA was isolated from cultures grown in 2 ml of YPD overnight at 30° using the Puregene Yeast Kit (Qiagen, Valencia, CA). Libraries for genome sequencing were created with dual indexing using 0.5–2.5 ng per reaction using a Nextera XT kit (Illumina). The libraries were multiplexed across six lanes of an Illumina HiSeq 2500 v4 sequencer using paired-end 125 bp output. Theoretical coverage of each library (assuming 100% full-length, high-quality reads) ranged from 52 to 352× (average 157×). Libraries of the LHL in wine must mostly failed to produce high-quality sequencing libraries, and those samples were excluded from further analyses. In most analyses we only considered a single clone from each of the eight *in vivo* populations, selecting the first numbered clone.

Reconstructing genotypic evolution: We analyzed two high-salt populations (AN-1 and BN-2) to estimate the genotype frequencies at the *ENA* locus over the course of evolution. From each of five time points (5, 10, 25, 50, and 100 passages) 50 clones were recovered from the frozen archive.

Clones were grown overnight on YPD agar and cells used for colony PCR (Blount *et al.* 2016). The primers ENA6-F and ENA6-R (Table S2) were used for PCR with GoTaq Green Mastermix (Promega, Madison, WI). The genotypes of the strains were distinguished using restriction enzyme length polymorphism (RFLP) of the PCR products by the restriction enzyme *Rsa*I, which cuts the 322134S allele but not the YPS128 or HN6 alleles. We also genotyped the terminal clones of the HHL and LHL beer wort evolved populations at the *MAL* locus subtelomeric region on the right arm of yeast chromosome II. We used two primer pairs to amplify genomic DNA of the terminal clones and digested the amplicons with a restriction enzyme whose sites were polymorphic between the two parental alleles (Table S2).

CRISPR-mediated LOH: We utilized CRISPR-Cas9 to induce double-strand breaks specific for alleles at target loci to induce LOH to homozygous states of either parent. The first target was near the *ENA* locus. CRISPR RNA (crRNA) were designed to target either the SSP24 or SSP253 parent of the HHL strain (SSP309). The gene region 5′ to the *ENA* locus encoding the *EHD3* and *KRS1* genes was targeted. A second target was the *MAL31* locus on chromosome II, where crRNA specific to either SSP309 parent were targeted. The crRNA were chosen such that the protospacer adjacent motif was different between the two alleles, and 1–7 bp of the 20 bp crRNA were different (Table S2). We used pML104-HygMx4, a derivative of pML104 (Laughery *et al.* 2015) designed to encode hygromycin resistance (gift from P. Wittkopp laboratory). crRNA oligos were cloned into *Bcl*I *Swa*I double-digested plasmid according to Laughery *et al.* (2015). Yeast transformation was done using a standard LiAc protocol (Gietz and Schiestl 2007) with cells of the ancestral genotype (SSP309). After an overnight recovery period at 4° following heat shock, cells were plated onto YPD + hygromycin B (200 mg/liter). Putative transformants were isolated and genotyped at five loci on chromosome IV or two loci on chromosome II (Table S2) via colony PCR-RFLP to determine if they had become homozygous and the chromosomal extent of homozygosity. Strains that had the appropriate LOH events were investigated for their growth rates following removal of the plasmid through serial transfer in liquid YPD every 12 hr for a total of 24–36 hr, followed by isolation of clones on YPD and testing for plasmid loss by streaking on YPD + hygromycin B plates.

Oxford nanopore long PCR sequencing: Long PCR products for the *ENA* locus were generated using primers anchored in the flanking genes (*KRS1* and *RSM10*; Table S2). We amplified genomic DNA of SSP253 using LATaq (Takara Bio.). Adapters for Nanopore sequencing were ligated onto the amplicon using the Ligation Sequencing Kit (SQK-LSK109), and the samples were run on a MinION (R9.4.1 FLO-MIN106) using MinKnow version 3.1.19. The resulting DNA library was loaded onto an R9.4.1 FLO-MIN106 flow cell on the ONT MinION device for sequencing until ~1100 sequences of the amplicon were generated. Basecalling was conducted using ONT Guppy software version 2.3.7. Quality filtering ($Q > 5$) was done using NanoFilt 2.3.0 (De Coster *et al.* 2018), and assembly was conducted using Canu 1.8 (Koren *et al.* 2017). To correct errors in the ONT contig, we assembled the Illumina short reads from SSP253 using the ONT contig as reference using bwa mem 0.7.8 (Li and Durbin 2009), and a consensus ONT-Illumina hybrid sequence for the SSP253 was extracted using bam2cns from the proovread pipeline (Hackl *et al.* 2014).

Data analysis

Variant calling using genomic sequences: The 125 bp paired reads were trimmed for quality and to remove Nextera adapters using Trimmomatic 0.36 (Bolger *et al.* 2014) in paired-end mode with the following flags: HEADCROP:12 LEADING:33 TRAILING:24 SLIDINGWINDOW:4:26 ILLUMINACLIP:NexteraPE-PE.fa:3:30:10 MINLEN:50. The genomes of the three parental haploid strains were assembled using Velvet Optimizer 2.2.4 (https://github.com/tseemann/VelvetOptimiser) running velvet 1.2.10 (Zerbino and Birney 2008). The genome assemblies were then aligned and used to create a vcf file of expected variants relative to S288c using Harvest (Treangen *et al.* 2014). The trimmed reads of libraries from the parental strains and evolved clones were then aligned to the S288c genome using bwa-mem (Li 2013) with default parameters. We used Picard 1.79 (http://broadinstitute.github.io/picard/) and GATK 4.0 (McKenna *et al.* 2010) using the recommended best practices of GATK (https://software.broadinstitute.org/gatk/best-practices/?v=3) to predict high-quality variants. The file of expected variants based on alignment of the parents was used for base recalibration using GATK's BaseRecalibrator, and variants were predicted using HaplotypeCaller. After plotting the distribution of mapping quality statistics across an initial combined dataset of SNPs, the resulting variants were filtered using VariantFiltration with the following parameters: "BaseQRankSum < -5.0 || BaseQRankSum > 5.0 || DP > 15000.0 || MQ < 59.0 || QD < 5.0 || FS > 5.0 || ReadPosRankSum < -5.0 || ReadPosRankSum > 5.0 || SOR > 5.0."

For each of the unfiltered SNPs, the mean depth per library was 83.3 [±38.4 (1 SD)]. For nonfiltered SNPs, genotypes were set to unknown when their depth was <20 or the genotype quality was <99. We also ran a separate mutation screen with relaxed quality parameters without filtering on parental allelic states to identify new mutations occurring during passaging using the criteria that they were absent in both parents and ancestral diploid strain and appeared with depth >20 and genotype quality ≥99. In analysis of LOH patterns, we removed all SNPs that were not present as alternate alleles in the parental strains and heterozygous in the ancestral genotype before passaging. SnpEff 4.3 k (Cingolani *et al.* 2012) was used to assign functional information to every SNP found between the parents. Indels were ignored for considering LOH, which underestimates the overall

amount of LOH and allelic diversity, but should not cause systematic biases in patterns.

We identified aneuploidy and copy number variation (CNV) using the software Control-FREEC v11.4 (Boeva *et al.* 2012). We used the *S. cerevisiae*–optimized parameters according to Steenwyk and Rokas (2017), except that window = 5000 bp.

Statistical analyses: All analyses and plots were created in R 3.4.4 (R Core Team 2019) unless otherwise specified. Most statistical tests utilized the base package; we also used the functions dunnTest in libraries FSA (Ogle 2018) and ggplot2 (Wickham 2009) and gridextra for graphical output (Auguié 2017).

Data availability

Strains and plasmids are available upon request. Figures S1–S6, Tables S1–S4, and vcf files are available at FigShare. The full pipeline, including scripts and data sets used for analysis of the genomic data, additional data files, and code for reconstructing figures, can be found on GitHub (https://github.com/Michigan-Mycology/Saccharomyces-LOH-paper/). Raw sequence data has been deposited into the National Center for Biotechnology Information Sequence Read Archive under BioProject PRJNA540143, with the accession numbers SRR8981718–SRR8981795. Supplemental material available at FigShare: https://doi.org/10.25386/genetics.9118316.

Results

SNPs in ancestral heterozygous genotypes

Our evolution experiments were initiated by creating two ancestors with two different but high levels of heterozygosity exceeding that common in most domesticated or wild *S. cerevisiae* strains (Liti *et al.* 2009; Duan *et al.* 2018). Genome sequence comparison of the ancestors of the HHL revealed 107,695 total high-quality heterozygous SNPs (Table 2). The majority of SNPs were in gene regions (67%), and synonymous SNPs were >2× as common as missense. The LHL ancestor was heterozygous at 54,460 positions, with similar ratios of functional categorization of the SNPs (Table 2). The expected distance between SNPs that change amino acid sequence (missense, nonsense, *etc*.) was 523 bp in HHL and 1043 bp in LHL.

Spectrum of LOH and CNV events

Following 100 days of serial passaging of replicate populations in multiple media types or 20 passages through waxworm larvae, we analyzed 70 individual clones to detect LOH events and mutations. Genome resequencing showed that most clones had undergone LOH, but that the LOH varied widely across environments and clones (Figure 1, Figure 2, and Figure S1). The average number of events per clone was 5.2 (median = 4; range = 0–46), effecting an average of 847 kb (median = 620 kb; range = 3.4–2750 kb) per clone (Figure 3). There was no evidence that LOH events encompassed entire chromosomes. The distribution of LOH sizes showed a mean of 121 kb (median = 7891 bp) with LOH events as small as 1 bp (theoretical minimum size) and as large as 1.1 Mb (Figure S2). The data on LOH length was bimodal with many events between 1 and 10 kb and another cluster between 100 and 1000 kb. The number of LOH events and total LOH bases were similar between evolved populations of the two genetic backgrounds ($P = 0.82$ and $P = 0.71$, respectively; Wilcoxon rank sum test). In contrast, environment significantly affected both number of LOH number events and total bases ($P = 0.04$ and $P = 0.0002$, respectively, Kruskal–Wallis test), implying environment had a greater influence on LOH than genetic background. Canavanine, high-salt, and larval environments revealed more LOH bases and typically had a larger number of LOH events than beer wort and YPD (Figure 3).

The characterization of SNPs undergoing LOH into functional sites is shown in Table 2 for both ancestral strains. There were fewer homozygous bases in the genic categories relative to intergenic. However, the observed distribution of LOH effects across functional sites was not distinct from the random null expectation for either the HHL (Fisher's exact test, $P = 0.39$) or the LHL ($P = 0.84$). Moreover, the distribution of which parental allele occurred in homozygous state was not distinguishable from the null hypothesis of random, *i.e.*, 50% each type [HHL: $t(35) = 0.038$, $P = 0.97$; LHL: $t(18) = -0.81$, $P = 0.43$], suggesting no tendency to become homozygous toward any genomic background.

Analysis of CNV and aneuploidy corroborated the absence of monosomies; however, 25 partial and complete trisomies were observed across the strains (Figure S3). All of the trisomies occurred in beer wort, canavanine, and high-salt environments, with trisomy particularly common on chromosome IV. All strains with clear trisomies of chromosome IV that were evolved in the high-salt environment were also strains with long-distance LOH, but not all LOH clones displayed trisomy. Both partial chromosome duplication and loss were observed, such as repeated partial monosomy of the right arm of chromosome XIV in an HHL canavanine environment.

New mutations

We identified 139 new single nucleotide mutations in the 54 evolved lines (46 *in vitro* and 8 *in vivo*). The average number of mutations per clone (2.6) was half that of the number of LOH events per clone (5.2). Under the expectation that 11 out of 12 of the canavanine-evolved strains would show a mutation at *CAN1* based on LOH patterns (Figure 1 and Figure 2), we assumed that some mutations were missed in this analysis because only seven out of 12 strains revealed mutations. Using less-stringent quality filtering and inclusion of indels, a total of 334 putative mutations could be detected in the evolved lines; however, these contained a larger proportion of loci showing

Table 2 Observed numbers of SNPs in the parental diploid genotypes by functional category and the average LOH SNPs observed and expected for the high heterozygosity lines (HHL) and low heterozygosity lines (LHL)

Functional category	Observed SNPS (HHL)	Observed SNPS (LHL)	Average LOH SNPS (HHL)	Expected LOH SNPS (HHL)	Average LOH SNPS (LHL)	Expected LOH SNPS (LHL)
Synonymous	48,422	25,122	2380.0	2289.3	1440.8	1399.3
Intergenic	36,075	17,705	1601.3	1705.6	938.5	986.2
Missense	22,916	11,489	1098.4	1083.4	648.4	640.0
Nonsense	156	71	7.1	7.4	2.7	4.0
Stop lost	58	38	2.4	2.7	1.6	2.1
Start lost	39	25	1.1	1.8	0.8	1.4
Intronic	22	9	0.8	1.0	0.6	0.5
Splice acceptor variant	4	0	0.2	0.2	0	0
Noncoding exon	3	1	0.3	0.1	0	0.1
Total	107,695	54,460	5,092.6	5,092.5	3,033.4	3,033.6

identical mutations across clones, which we interpret as likely false positives (14% *vs.* 6% in the more conservative set). With the more liberal set, however, we were able to detect 10 out of 12 strains as showing independent *CAN1* mutations.

Using the conservative set going forward, most ($n = 126$; 91%) of the mutations were found in a heterozygous state, and only 13 (9%) were homozygous. The genome-wide rate of LOH was 7% of the genome, making the observed number of homozygous mutations not statistically distinguishable from the random expectation (exact binomial test, $P = 0.25$). Most of the mutations were likely functionally impactful (54% missense and 8% nonsense *vs.* 22% synonymous and 16% intergenic). The 131 single nucleotide mutations fell into 113 genes or intergenic regions. Seven genes showed more than one functionally impactful, parallel mutation (*e.g.*, missense and nonsense), implying a fitness advantage to the mutations (Table S3).

Fitness of evolved clones

The fitness of the *in vitro* evolved clones relative to their ancestor was estimated with three measures: growth rate in exponential phase, efficiency of growth (EOG), *e.g.*, the maximal optical density of saturated cultures, and relative competitive ability when coinoculated with a common strain. A relative fitness >1 implies clones evolved higher fitness. Only for the high-salt media were consistent, positive relative fitness changes observed across all measures (Figure 4). However, the three measures were all highly positively correlated [Pearson's correlation: growth rate *vs.* EOG, $r = 0.53$, $t(58) = 4.8$, $P < 1.0e{-}4$; growth rate *vs.* competition, $r = 0.58$, $t(58) = 5.4$, $P < 1.0e{-}5$), and EOG *vs.* competition, $r = 0.62$, $t(58 = 6.1$, $P < 1.0e{-}6$]. Of the 13 measurements × environment, five of the mean fitness estimates of the evolved were statistically distinct depending on ancestral genotype ($P < 0.01$, Welch two-sample *t*-test). We also estimated the fitness of 20 clones after 20 passages in *G. mellonella* 20 using a competition assay. The estimated fitness of the 20 *G. mellonella* passaged clones was surprisingly lower than that of the ancestral strain for all but one clone (Table S4).

Evidence for selection acting on LOH

Our experimental design allows us to test loci for significant differences in direction of LOH, *i.e.*, toward a particular parental allele, loci with increased amounts of LOH, or loci whose function may be implicated in the particular habitat.

Nonenvironment-specific LOH patterns: Only one chromosomal location showed evidence of selection favoring a particular allele regardless of environment (Fisher's exact test, $P = 0.05$): the chromosome XII region containing the ribosomal RNA repeat in the HHL strains, where a homozygous genotype of the Chinese allele repeatedly was observed (Figure 1). Eight strains demonstrated a homozygous genotype for the majority of the chromosome distal to the ribosomal RNA array, in each case representing the Chinese genetic background. For the LHL, four out of 19 strains displayed LOH at this region, but no particular allele appeared favored (Figure 2).

Environment-specific LOH patterns: *Beer wort:* No significantly overrepresented LOH regions were observed. Two strains showed atypical increases in fitness measured by EOG (Figure 4B). Both of these strains showed mapping of reads indicative of LOH in the subtelomeric region of the right arm of chromosome II, which has multiple genes involved in maltose metabolism (Figure S4A). For one of the two genotypes we were able to confirm loss of the nonclinical parent's alleles by PCR-RFLP analyses (Figure S4B). The effect of homozygosity of the *MAL31* locus in the HHL background was tested using CRISPR-mediated LOH. Comparison of homozygotes of the SSP253 (Clinical) allele with the homozygotes of the SSP24 (Chinese) allele revealed a nonsignificant fitness increase in EOG of the Clinical allele homozygotes compared to the Chinese allele homozygotes (4%; $P < 0.093$, Wilcoxon rank sum test). Additional experiments will be needed to characterize the LOH events in this highly repetitive subtelomeric region.

Canavanine: The major region identified as significantly enriched for LOH events in a canavanine environment-specific

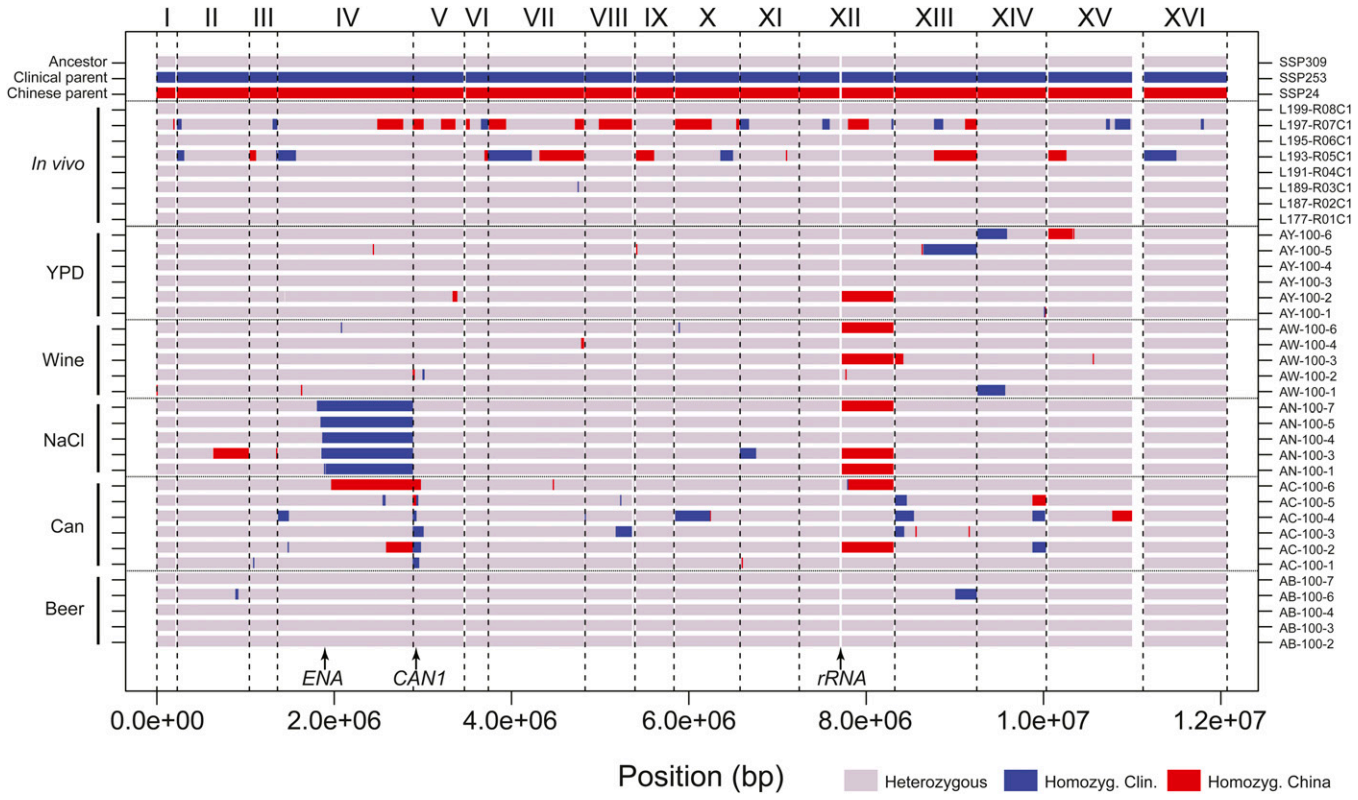

Figure 1 Overview of LOH across HHL evolved clones across the 16 *S. cerevisiae* chromosomes. Each sample represents an individual clone sequenced from an independent population with environment indicated and mapped to the S288c genome. Shown are genotypes at 10 kb resolution, plotting the majority genotype across SNPs. For the eight *in vivo* populations, only the first clone is shown. White regions represent unmapped, typically repetitive regions of the S288c genome, and are not shown to scale.

manner was the *CAN1* subtelomeric region of chromosome V of both backgrounds (HHL: $P < 10^{-5}$; LHL: $P < 0.005$) (Figure 5). Only one of the 12 strains maintained heterozygosity at the *CAN1* locus, and this strain (BC-100-8) had the lowest relative fitness estimated for the LHL canavanine-evolved strains. Chromosome IV, beginning at ~1.0 Mb, showed a preponderance of the oak parent allele in the LHL background (Figure 2), but the pattern was not significant ($P = 0.08$). Strain AC-100-6 demonstrated a single base pair LOH event (maximum size 310 bp) in the *ARG3* gene at amino acid position 175. The evolved line converted a Lys-Asp heterozygous polymorphism to a homozygous Asp genotype.

High salt: A single region was identified as significantly enriched for LOH events in a high-salt–specific manner that spanned a large portion of chromosome IV, including the *ENA* sodium and potassium exporting ATPase locus (HHL: $P < 10^{-5}$; LHL: $P < 0.1$) (Figure 1 and Figure 6). Only three out of six LHL lines demonstrated LOH at or near the *ENA* locus and extending to the telomere, but all six HHL lines demonstrated homozygosity. Moreover, in each case, the locus became homozygous for the allele from the clinical parent. The *ENA* locus is well known as possessing genetic variation associated with high-salt tolerance (Daran-Lapujade *et al.* 2009; Anderson *et al.* 2010; Sirr *et al.* 2018). CNV of *ENA* is observed, with one to three copies typical of most strains of the wine/European lineage associated with higher tolerance to salt and other ions (Warringer *et al.* 2011) (Figure S5). We explored the underlying structure of the *ENA* region in the parental strains using a combination of genome assembly analysis and long-range PCR followed by sequencing using Oxford Nanopore Technology. We determined that the clinical parent SSP253 (from the UK) has two copies of the *ENA* locus, whereas both strains SSP24 and SSP264 have only a single copy (Figure S5). Our phylogenetic analysis confirms the hypothesis that multiple *ENA* gene copies at the *ENA* locus derive from introgression from *S. paradoxus* (Doniger *et al.* 2008). We estimated the growth rate of the ancestral haploids and found that indeed SSP253 had a significantly higher growth rate than both SSP24 and SSP264 in high-salt media (Figure 7A). In the next section we explore the specific fitness effect of the LOH and track its rise through experimental populations over time.

Wine must: No significantly overrepresented LOH regions were observed. One strain, AW-100-2, displayed a single base pair LOH in the upstream region of the gene *HPT1*, which is involved in the salvage pathway of purine nucleotide biosynthesis and known to function in the early stages of wine fermentation (Rossignol *et al.* 2003; Novo *et al.* 2013). A second strain, AW-100-4, was homozygous for the Chinese allele in the ~30 kb subtelomeric region of the right arm of

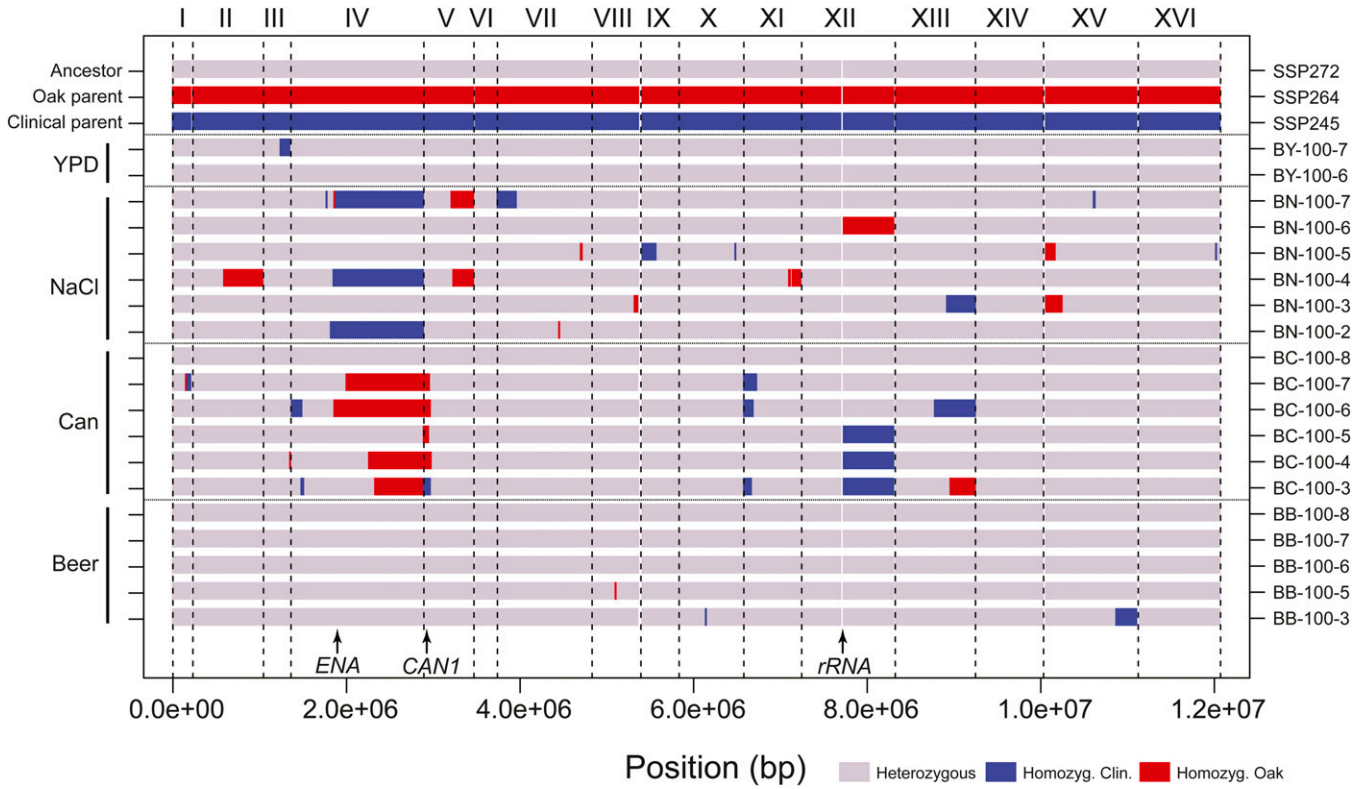

Figure 2 Overview of LOH across LHL evolved clones across the 16 *S. cerevisiae* chromosomes. Each sample represents an individual clone sequenced from an independent population with environment indicated and mapped to the S288c genome. Shown are genotypes at 10 kb resolution, plotting the majority genotype across SNPs. White regions represent unmapped, typically repetitive regions of the S288c genome, and are not shown to scale.

chromosome VII. This region contains the genes *MAL11*, *MAL12*, and *MAL13*, which are known to be associated with lower copy numbers in wine strains and whose deletion improves fitness in a fermentation environment (Steenwyk and Rokas 2017).

YPD: No significantly overrepresented LOH regions were observed. One strain, AY-100-4, was homozygous for the Chinese allele for a 3991 bp conversion event specifically encompassing the *FLO8* gene, its upstream region, and a small portion of the 5′ neighboring gene, *KAP123*. Flo8 is involved in flocculation and pseudohyphal growth and has been implicated in adaptation to long term experimental culture (Hope *et al.* 2017). The likelihood that this LOH event was driven by selection is considerable, because the clinical parent encodes a *FLO8* allele with a nonsense mutation [W142* (TGG→TAG)] that produces a largely truncated version of the Flo8p protein, whereas the Chinese parent shows a wild type length protein. The nonsense mutation of 322134S (SSP24) was identical to the one previously reported in S288c that leads to inability of the strain to grow in pseudohyphal form or flocculate (Liu *et al.* 1996). This mutation, therefore, may not be lab derived as previously assumed, but may be selected against during long-term growth near saturation or in a chemostat.

Larvae: No significantly overrepresented LOH regions were observed. We found six out of 24 of the clones sequenced showed independent LOH (primarily gene conversion-like) events at the *VMA1* locus suggestive of conversion of the intein-less Chinese parent allele to an intein-containing clinical parent allele. Gene conversion favoring spread of inteins at *VMA1* catalyzed by the targeting of the homing endonuclease of the intein-containing allele to intein-less alleles has previous been reported, although its effect was hypothesized to be meiosis-specific (Gimble and Thorner 1992).

Dynamics of the major effect LOH genotype in high salt

We hypothesized that LOH at the *ENA* locus on chromosome IV was a primary driver of adaptation to a high-salt condition. We predicted that the homozygous genotype from the clinical parent with two gene copies would rise to high frequency early during the course of evolution and that clones with the LOH genotype would have a higher fitness than those with the ancestral heterozygous genotype. To test this, we genotyped the *ENA* locus from 50 clones isolated from the archived populations of one HHL and LHL line at multiple time points (5, 10, 25, 50, and 100 days). We also estimated the fitness of five clones with and without the LOH event for polymorphic time points.

The data revealed that the *ENA* homozygous genotype arose and reached high frequency relatively quickly, achieving fixation by the end of the experiment (Figure 7B). At all polymorphic time points, the fitness of random

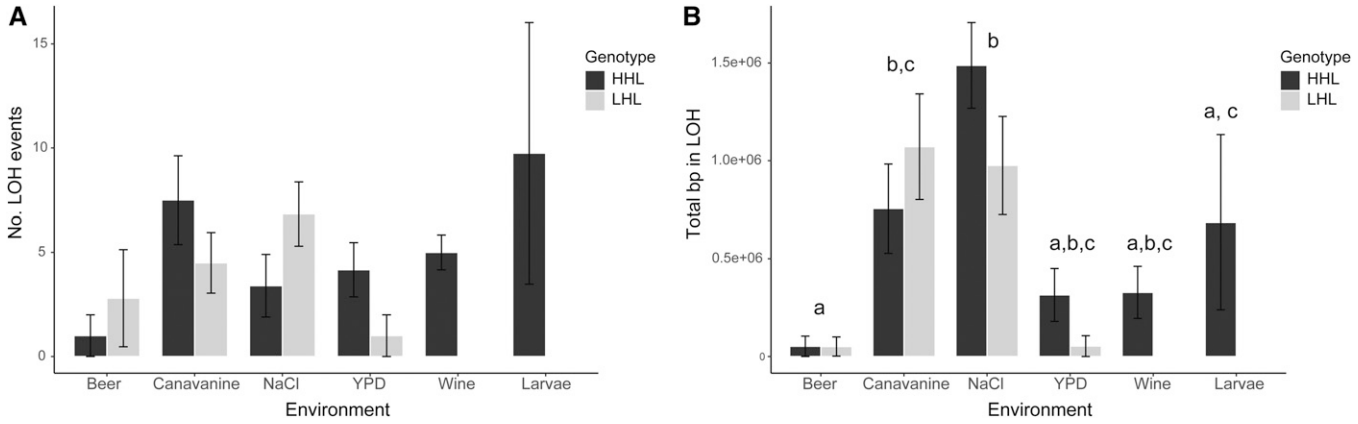

Figure 3 Number of LOH events (A) and total LOH base pairs (B) across environments for the two ancestral genotypes. Bars represent means across independent populations and error bars show SE. Wine and larval populations were not generated for LHL. Letters above bars indicate environments which are not statistically distinguishable ($P > 0.05$) by a Dunn test after adjusting *P*-values using the Benjamini–Hochberg method. No pairwise comparisons were significant for the number of events (A) following *P*-value adjustment. Tests were conducted using HHL and LHL genotypes combined.

clones with and without the LOH genotype, showed a clear fitness benefit estimated by growth rate for the homozygous genotype, with differences being most prominent at the beginning of the experiment (Figure 7C). Finally, the adaptation of the strains to the high-salt media appears to have a negative effect on fitness of the strains in canavanine and a neutral effect in the beer wort media (Figure 7D).

To isolate the specific effect of the *ENA* LOH event from the remainder of the genotypic changes occurring during experimental evolution, we attempted to reconstruct the change using CRISPR-induced LOH (Sadhu *et al.* 2016; Gorter de Vries *et al.* 2018). This approach takes advantage of the fact that CRISPR-Cas9 is able to induce allele-specific double-strand breaks that can be repaired using the other allele as a template, leading to gene conversion or crossing over. Using guide RNAs specific to variants in either the Clinical allele or the Chinese allele in the region 5′ to the *ENA* locus, we transformed the ancestral strain SSP309 and genotyped the resulting transformants at multiple markers along chromosome IV to determine the extent of LOH. The rate of LOH at guide RNA target site was high (96% and 86% for the SSP24 and SSP253 constructs, respectively). Of the genotypes that had undergone LOH at the target region, 33% and 18% for the SSP24 and SSP253 constructs, respectively, underwent a form of long-distance LOH that included the *ENA* locus (Figure S6). We then measured the fitness of variants engineered to have LOH at *ENA*, and found that the variants homozygous for the Chinese allele were significantly worse than the variants homozygous for the Clinical allele ($P = 0.004$, Wilcoxon rank sum test), with clinical homozygotes having a 27% relative fitness increase compared to the ancestral genotype. These data suggest that the observation of rapid rise of the homozygous genotype in the HHL populations was due to the specific fitness advantage of the homozygous clinical allele genotype.

Mechanism of LOH shows a majority of events to be gene conversion

We had hypothesized that the nature of the LOH events may be dependent on initial heterozygosity, and we therefore contrasted the underlying mechanisms leading to LOH in the HHL *vs.* the LHL. Because our study does not isolate reciprocal products of recombination, only a limited number of patterns can be observed, and the precise mechanisms are obscured. Six classes of events could be distinguished that correspond with different mechanisms of repair in the double strand break repair model (St Charles *et al.* 2012) (Figure 8A): (1) simple gene conversion in which a homozygous region is flanked by heterozygous sequences (*e.g.*, St. Charles types A-E); (2) complex gene conversion in which homozygous regions contain intervening heterozygous sequence (St. Charles type F); (3) complex gene conversion in which homozygous regions of two alternate homozygous states are present either adjacently or with intervening heterozygous DNA (St. Charles type G); (4) simple crossover without associated gene conversion (St. Charles type H1 and H2); (5) crossover with heterozygosity near the breakpoint (St. Charles type H3); and (6) crossover with associated gene conversion of varying complexity (St. Charles types I, J, and K). We also detected events that were associated with deletions as detected by CNV analysis (Figure S3). The majority of events were type 1 or simple gene conversion events. The second most predominant event was the type 4 event, a simple crossover event via double Holliday junction formation or break-induced repair. Crossing over with associated gene conversion was also observed, although less common (classes 5 and 6). Deletions primarily occurred in the canavanine clones, with three clones losing ~140 kb from one copy of the right arm of chromosome XIV, and two clones losing one copy of the left arm of chromosome V containing *CAN1*. There was no significant difference in the type of

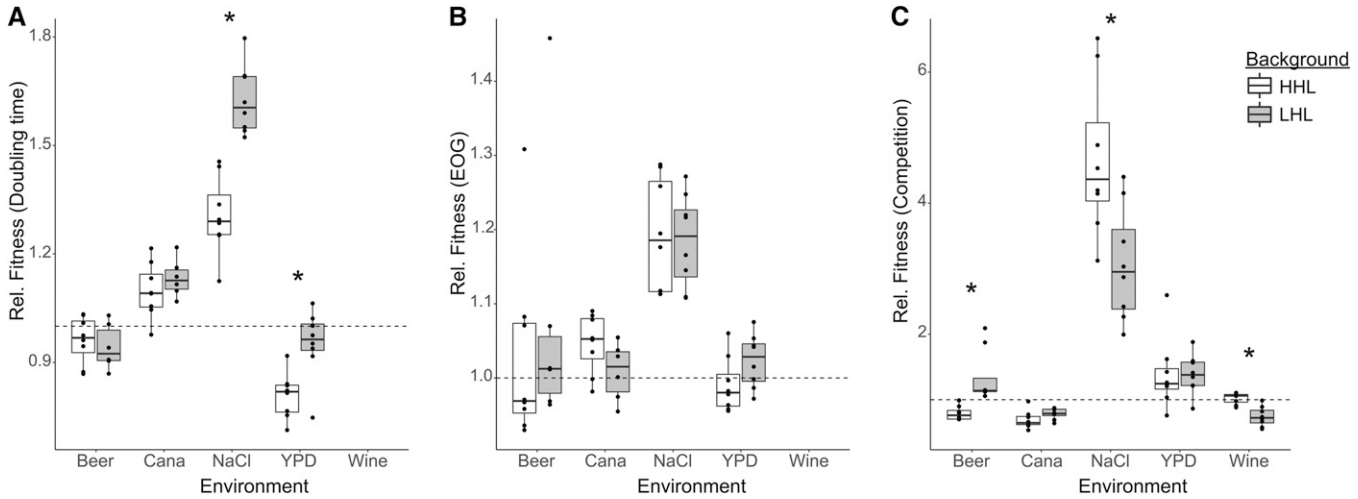

Figure 4 Fitness gain for each environment shows variation across measures and background genotype. Values shown are relative to ancestral genotype (dashed line). (A) Fitness as measured using doubling time. (B) Fitness measured using efficiency of growth (EOG) (*i.e.*, carrying capacity). (C) Fitness measured using relative competitive growth in the presence of a marked ancestral strain. Each dot represents an individual clone. Boxes indicate the 25–75% percentiles, bars indicate medians, and the whiskers extend to 1.5 × the interquartile range. Asterisks indicate environments/measures where there was a significant differences in fitness of evolved strains depending on genetic background ($P < 0.01$; Welch two-sample *t*-test). Wine strains were not tested by growth curve analysis.

LOH event and the LHL or HHL events ($P = 0.69$, Fisher's exact test).

LOH was unequal across the chromosomes; however, it was not correlated with chromosome size (HHL: $r(14) = 0.05, P = 0.86$; LHL: $r(14) = -0.33, P = 0.22$). The distribution of LOH events across chromosomes was not different between HHL and LHL populations ($P = 0.62$, Fisher's exact test).

Discussion

Here, we investigated the mechanism and significance of LOH occurring during the evolution of yeast populations to multiple environments. We used crosses of known haploid genotypes and high-coverage genome resequencing of evolved diploid clones, making it simple to accurately determine the locations of the inferred LOH events. Our study advances knowledge on the importance of LOH to evolution in three important ways. First, it samples three random *S. cerevisiae* genomes and asks whether LOH can create genetic variants of higher fitness to multiple, seminatural environments. We found ample evidence that this could occur, and by using different starting genotypes we determined that input genotype has a strong effect on which loci show LOH. Second, we tested how the initial heterozygosity influenced the mechanism and rate of LOH. Surprisingly, it did not, and this observation, in combination with LOH rates in comparable studies (Dutta *et al.* 2017; Marad *et al.* 2018) suggests an independence of LOH on sequence heterogeneity. Lastly, we demonstrate a method for engineering specific LOH events using CRISPR to facilitate robust testing of fitness consequences of individual LOH events. Overall, our findings suggest that LOH drives adaptation in heterozygous *S. cerevisiae* populations, and our system serves as a model for understanding the evolutionary implications of LOH in the numerous other asexual diploid organisms that are much less amenable in the laboratory.

Our experiment was specifically designed to identify adaptation by parallel LOH events, particularly those specific to an environment. Two primary regions showed significant environment-specific patterns: the *ENA* locus on chromosome IV in the high-salt environment and the *CAN1* locus on chromosome V in the canavanine environment. These two regions stand out as being clear cases in which the LOH event can be tied to function, because mutations or duplications of both genes are known to be involved in resistance in these two stressful habitats (Lang and Murray 2008; Anderson *et al.* 2010). In the case of *ENA*, we used CRISPR-mediated mitotic recombination to validate our hypothesis that the specific LOH at *ENA* was a driver of adaptation, and in combination with data showing a rapid fixation of the LOH genotype in two populations (Figure 7), it appears that the LOH event occurred in the earliest generations due to the high fitness it confers. In other environments, we did not observe much evidence of parallel LOH. At least two possibilities could explain this difference. First, the distribution of fitness effects of LOH events might vary for given environments or traits because of genomic architecture, making the probability of parallel evolution in some habitats more likely than others (Bailey *et al.* 2017). This would predict that traits linked to loci near hotspots of mitotic recombination, such as subtelomeric regions, would be more likely to show parallel LOH. Second, the fitness landscape for a particular environment could be relatively flat, meaning that there are few genotypic changes of large effect. This might be the case for environments like beer or wine, in which most *S. cerevisiae* genotypes are already well adapted to grow.

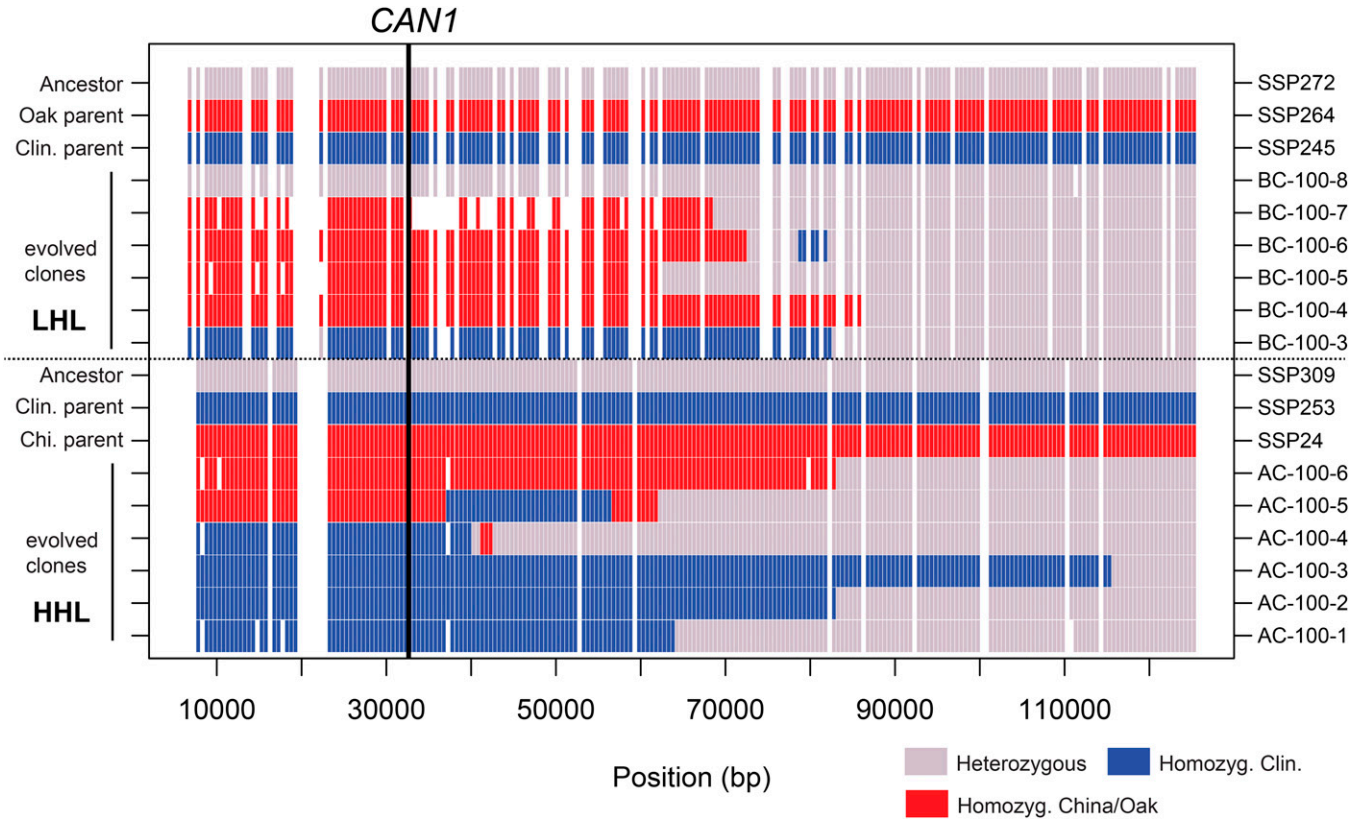

Figure 5 Overview of heterozygosity demonstrates LOH occurred at *CAN1* in most canavanine evolved lines. Shown is the region of chromosome V from the left telomere to 120 kb. Heterozygosity is shown as the dominant genotype frequency in windows of 500 bp. White gaps indicate regions that cannot be mapped uniquely, are not polymorphic between the two parental genotypes, or have mean coverage below the threshold.

We were particularly interested in testing whether the starting heterozygosity would affect the loci involved in LOH, the rate of LOH, and the adaptability (final change in fitness). Multiple studies now suggest that standing variation is more potent source of adaptation than *de novo* mutation (Burke *et al.* 2014; Vázquez-Garcia *et al.* 2017), even when that variation exists solely in the genome of a single diploid genotype (Smukowski Heil *et al.* 2017). This suggests that there is ample recessive or partially recessive variation for fitness in various environments when two divergent genotypes mate. Initial heterozygosity had little influence on the rate of LOH observed, with HHL lines showing 5.6 average LOH events per clone and LHL an average of 4.4 events per clone. After 100 days of evolution, LOH summed to ~1110 amino acid changing (missense and nonsense, *etc.*) SNPs per HHL clone and ~655 per LHL clone. This number is over two orders of magnitude than the ~2 amino acid replacement *de novo* mutations per clone. Clearly, the potential for LOH to influence the evolution of asexual lines is much greater than mutation. On the other hand, some of the LOH events are clearly associated with *de novo* mutations, such as at the *CAN1* locus, highlighting the dual function of LOH. LOH has likewise been observed in experimental yeast populations lacking initial heterozygosity as a mechanism by which *de novo* mutations become homozygous (Fisher *et al.* 2018; Marad *et al.* 2018).The ratio of heterozygous:homozygous new mutations observed in Marad *et al.* (2018) was very similar to that in which we observed in this study (8% *vs.* 9%). On the other end of the spectrum, *S. cerevisiae/S. uvarum* hybrids show only 80% nucleotide similarity at coding regions, yet the rate of LOH is approximately half that of *S. cerevisiae* heterozygotes (Piotrowski *et al.* 2012; Smukowski Heil *et al.* 2017). These data suggest that for natural ranges of heterozygosity of *S. cerevisiae*, the rate of LOH is constant.

There has been considerable effort to understand the distribution of fitness effects and trait variation in *S. cerevisiae*, with evidence that there is extensive genetic variation for most traits across the species shaped by population structure and genetic drift (Doniger *et al.* 2008; Warringer *et al.* 2011). Much of this variation is attributable to differences in gene content or CNV (Bergström *et al.* 2014; Peter *et al.* 2018). In the case of *ENA*, both sequence diversity and gene copy number likely influence the fitness of the genotype in high salt. We saw less frequent LOH of the *ENA* locus in the LHL line with the oak parent mated to the favored allele (clinical), than in the HHL line with the Chinese parent mated to the favored allele. The oak parent (SSP264) is more fit in high salt than the Chinese parent (SSP24; Figure 7A), despite having a very similar amino acid sequence (Figure S6). We identified a change in the cyclic AMP response

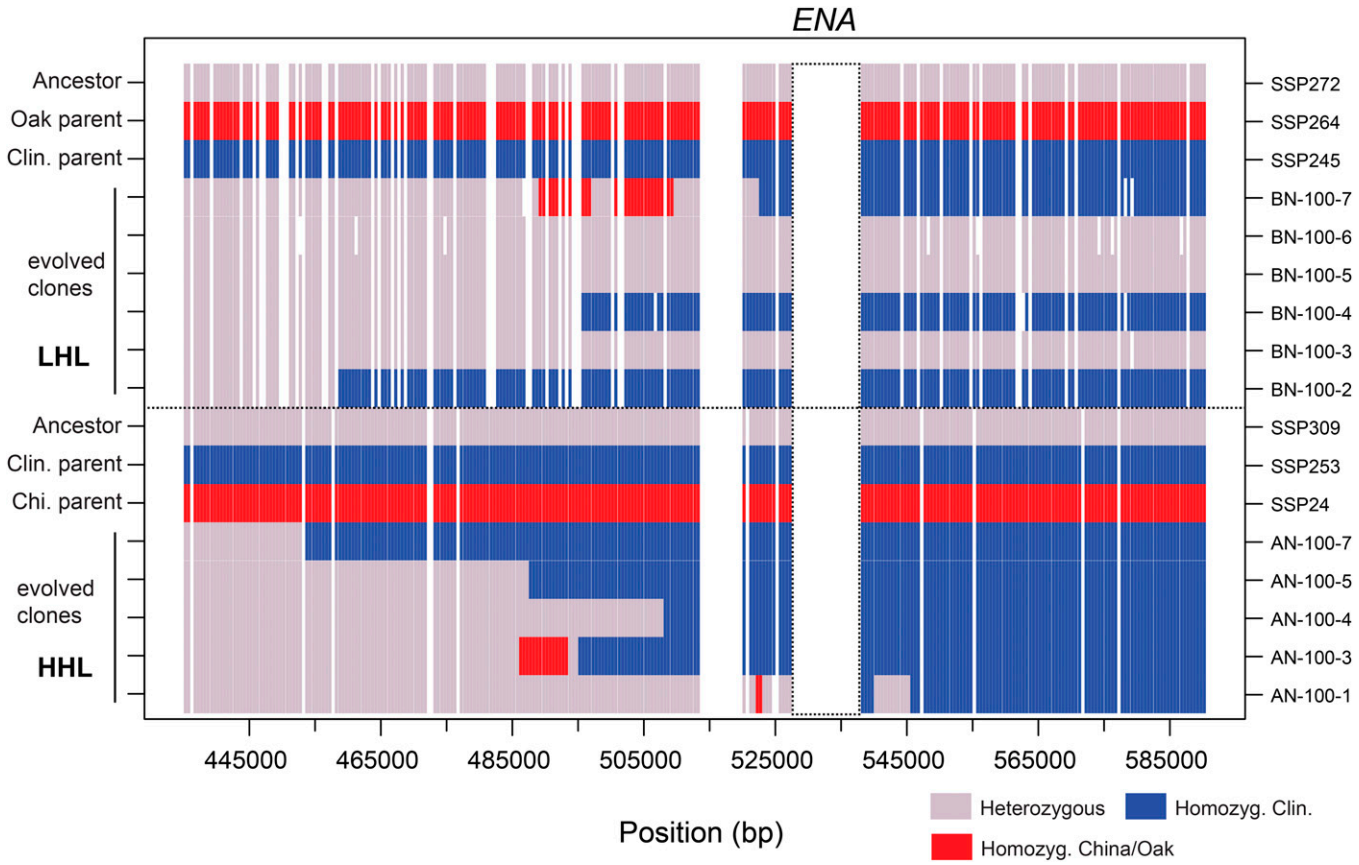

Figure 6 Overview of heterozygosity demonstrates extensive LOH favoring the allele from the clinical parent at the *ENA* locus in most high-salt evolved lines. Shown is the region of chromosome IV from 435 to 590 kb. Heterozygosity is shown as the majority genotype frequency in windows of 500 bp. White gaps indicate regions that cannot be mapped uniquely, are not polymorphic between the two parental genotypes, or have mean coverage below the threshold.

element of the *ENA* promoter region specific to SSP24 that may explain its phenotype. The SSP24 promoter sequence diverges from the canonical sequence such that the underlined cytosine of the consensus element sequence is mutated to adenine (TGACGTTT → TGAAGTTT). The cyclic AMP response element is bound by the repressor Sko1 that is regulated by the high-osmolarity glycerol pathway (Ruiz and Arino 2007; Sirr *et al.* 2018).

It is particularly striking that the *ENA* and *CAN1* LOH events are exclusively associated with crossing over rather than gene conversion in both genetic backgrounds (Figure 5 and Figure 6). One hypothesis is that antirecombination mechanisms inhibit gene conversion at a local region and favor resection and homology search at a distant site (Datta *et al.* 1996; Symington *et al.* 2014). A simpler hypothesis is that LOH by crossing over is faster than gene conversion, because it can be generated from nonspecific, distal, double-strand breaks. Our results with CRISPR-induced double-strand breaks near the *ENA* locus show gene conversion to be more common than crossing over, suggesting that there are no physical limitations favoring crossing over (Figure S6). When long-distance LOH occurs, it is likely to involve multiple sites of consequence to fitness of the strains, making the LOH event highly pleiotropic. This type of LOH is potentially limiting with respect to future adaptation, and it would be interesting to test whether short distance LOH strains could adapt more readily to a different environment than long-distance LOH genotypes. A third hypothesis for the frequent demonstration of long-distance LOH at the *ENA* locus is that there may be multiple loci displaying positive epistasis on chromosome IV that would favor long-distance LOH. The three alternatives could be readily tested with CRISPR methodology.

Because populations were kept at a large effective size, it is likely that the majority of LOH events were either selectively beneficial or nearly neutral. This differs from previous studies which used serial propagation of single clones (mutation accumulation) and may have contained highly deleterious LOH events (Dutta *et al.* 2017; Sharp *et al.* 2018). Dutta *et al.* (2017) performed a mutation accumulation study of vegetatively propagated diploids for 1140 generations. They found 2–35% of the genome became homozygous, with 7.3 events per clone (excluding possible abortive meiosis genotypes) and an average of three mutations per clone. We found similar results after ~500 generations with a range of 0–23% genome-wide LOH, 5.6 LOH events, and ~3 of mutations

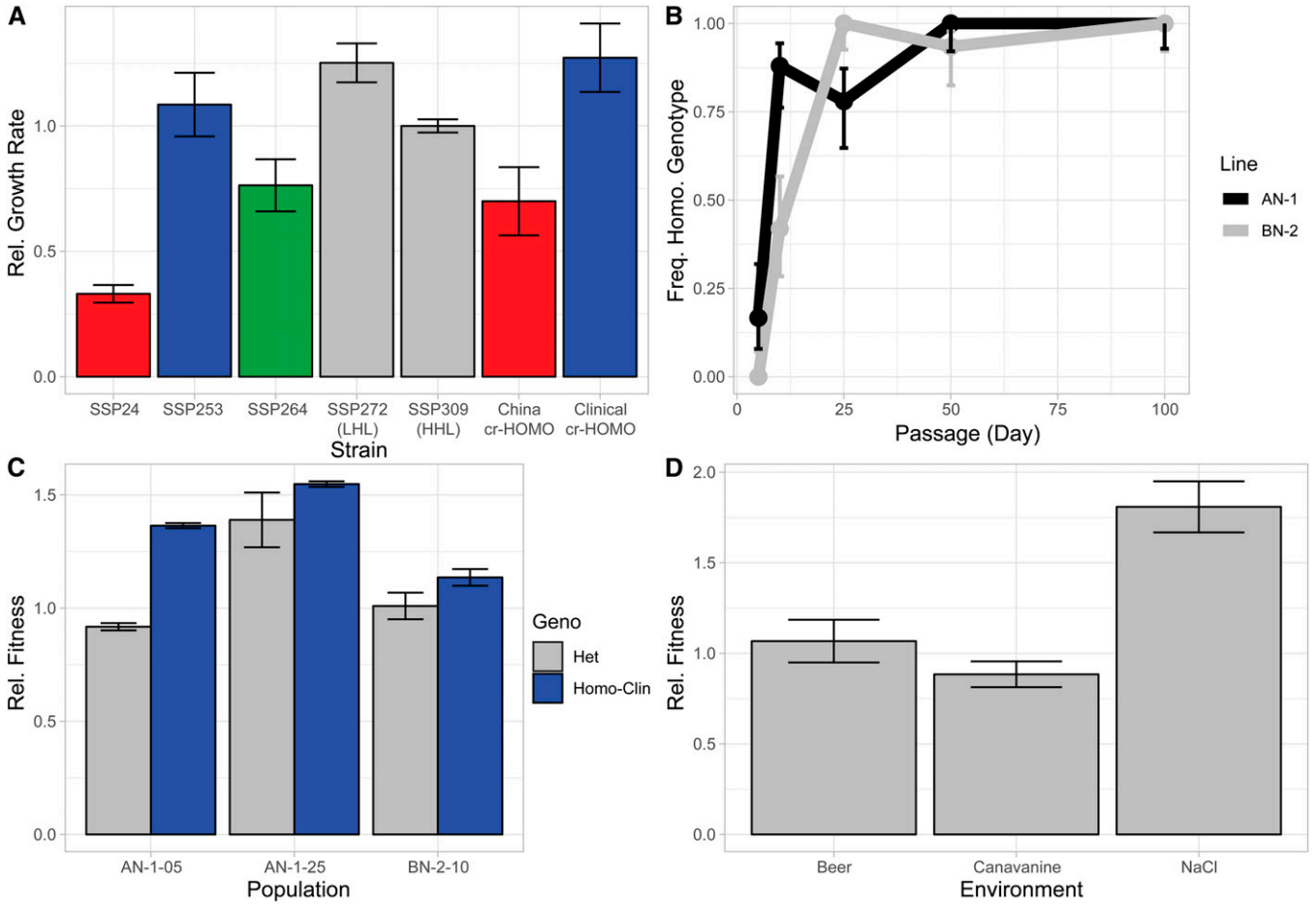

Figure 7 Rapid appearance of LOH genotype homozygous for *ENA* clinical allele in high-salt environment is associated with fitness increase measured by growth rate. (A) Initial ancestral haploids [SSP24 (Chinese parent), SSP253 (clinical parent), SSP264 (oak parent)] and diploids [SSP272 (LHL ancestor), SSP309 (LHL ancestor)], and CRISPR-mediated LOH transformants [China-cr-HOMO (homozygous for SSP24 *ENA* allele), Clinical-cr-HOMO (homozygous for SSP253 *ENA* allele)] show a marked difference in growth rate in salt. Values shown are relative to SSP309. Error bars indicate ±1 SD across replicate cultures or independent transformants. (B) Frequency of the homozygous genotype at the *ENA* locus over time; 36–50 clones per time point were used. Error bars indicate confidence intervals based on binomial distribution. AN-1 is one population of HHL and BN-2 is a population of LHL. (C) Relative fitness of strains with (Homo-Clin) and without (Het) LOH *ENA* genotype at intermediate time points. Fitness is relative to the ancestor. Error bars indicate ±1 SD across clone means. AN-1 population time points at 5 and 25 days are shown, and BN-2 population is shown at time 10 days. (D) Relative fitness of individual clones derived from six independent 100-day populations grown in high salt are shown across three media types. Error bars indicate ±1 SD across clone means.

per clone. The surprising similarity between rates of LOH in the present study and in mutation accumulation studies could be explained if the impacts of LOH on fitness are generally neutral. Further study on the distribution of fitness effects of LOH events is warranted. In classifying LOH into types of events, we found gene conversion to be more common than crossing over, similar to what is observed in laboratory assays devoid of selection (Dutta *et al.* 2017; Zhang *et al.* 2019) as well as populations evolving under selection (Vázquez-Garcia *et al.* 2017). We found that most LOH events (presumably crossovers) that extended to the telomere were not associated with gene conversion (Figure 8), which is expected because our system can only detect half of conversions resulting from a G1 double-strand break (St Charles *et al.* 2012). The median length of each LOH event in this study was ~8 kb, which is lower than that in a mutation accumulation study (17 kb) (Dutta *et al.* 2017) or in gene conversion tracts associated with crossing over (9–13 kb; St Charles *et al.* 2012; Zhang *et al.* 2019). These studies with *S. cerevisiae* paint a rather consistent picture of sizes, mechanism, and even location of LOH events. There appear to be a few consistent LOH hotspots detected postlaboratory evolution. A hotspot on the right arm of chromosome IV is frequently observed (Smukowski Heil *et al.* 2017; Zhang *et al.* 2019). The ribosomal RNA containing chromosome (chromosome XII) also appears to be a hotspot for LOH (Fisher *et al.* 2018), which we also found to be a hotspot of nonenvironment-specific LOH in the HHL lines. These two hotspots correspond with what is observed in natural populations of yeast revealed from population genomics (Magwene *et al.* 2011; Peter *et al.* 2018), and correspond with the two longest arms in the *S. cerevisiae* genome

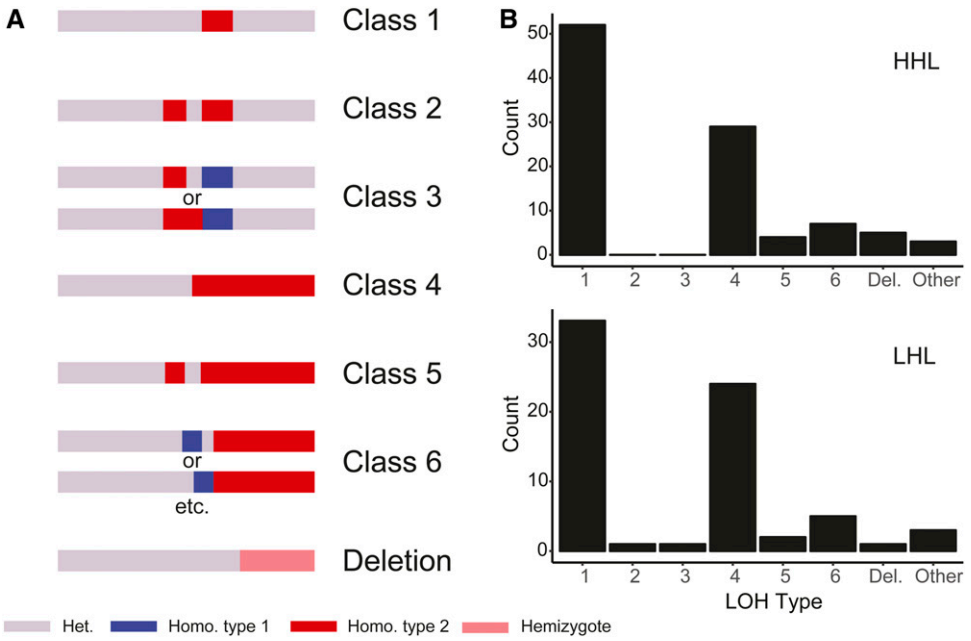

Figure 8 Approximately half of LOH is generated from gene conversion-type events. (A). Clones displaying LOH can be classified according to their patterns, following St Charles *et al.* (2012). (B). These patterns show gene conversion to be the predominant mode of LOH, and the pattern does not differ dependent on initial host genotype. Two strains, L193-R05C1 and L197-R07C1, were not included due to their unusual patterns of LOH suggestive of meiosis or abortive meiosis.

which are known to be hotspots of LOH in the laboratory (McMurray and Gottschling 2003).

LOH in *S. cerevisiae* appears to differ in a number of ways from the clinically important yeast *Candida albicans*, which has been a key model for studies of phenotypic impacts of LOH in fungi (Forche *et al.* 2011; Ciudad *et al.* 2016). LOH is critically important for *C. albicans* because it is diploid and more clonal than *Saccharomyces* (Nieuwenhuis and James 2016). Aneuploidy appears to be a common route to rapid adaptation in *C. albicans*, and both trisomy and monosomy of particular chromosomes provide a route to fitness increase (Selmecki *et al.* 2006, 2010). On the other hand, like *S. cerevisiae*, wild isolates of *C. albicans* generally lack whole chromosome LOH (Hirakawa *et al.* 2015; Ropars *et al.* 2018). We found no instances of LOH by whole chromosome aneuploidy in our experiment, and this is consistent with other studies that found gain of chromosome copy number to be much more common than loss for diploids (Zhu *et al.* 2014; Sharp *et al.* 2018). A recent experimental evolution study of *C. albicans* showed that like *S. cerevisiae*, LOH is dominated by gene conversion, with LOH events much smaller in *C. albicans* on average and long-distance LOH events even rarer (Ene *et al.* 2018). Ene *et al.* (2018) also found a high amount of *de novo* mutation associated with LOH breakpoints, which has also been reported during mitotic recombination in *S. cerevisiae* (Hicks *et al.* 2010; Deem *et al.* 2011) but was not observed in our study. Three strains in the larval passaging (L193-R05C1, L195-R06C2, L197-R07C1) did, however, have a large number of LOH regions, but we interpret these outlier strains as resulting from aborted meiosis followed by resumption of vegetative growth (*e.g.*, Laureau *et al.* 2016; Dutta *et al.* 2017) or meiosis followed by intratetrad selfing. Multiple forms of stress increase LOH in both species, consistent with the increased number of double-strand breaks (Forche *et al.* 2011; Rosen *et al.* 2013; Zhang *et al.* 2019). However, we did not observe an increase in LOH *in vivo* as has been observed in *C. albicans* (Forche *et al.* 2009), which may be due to *Galleria* being a poorer model host relative to mouse or the endothermic *vs.* exothermic nature of the hosts.

These results paint a picture of broad adaptive significance of LOH in mitotically dividing diploid populations. A more detailed analysis is warranted of the fitness effect of individual events and the proportion of them that are neutral, environment-specific, or deleterious relative to their physical size. We show CRISPR to be an efficient tool for generating and isolating fitness effects individual LOH events. We found a very high conversion rate using the tool and additional developments are underway to recreate more precise events using multiplexed guide RNAs (Stovicek *et al.* 2017). Additional genotypes sourced from different natural environments and other selective environments would be useful to paint the full picture of *S. cerevisiae* diversity and how the frequency and nature of epistatic interactions and dominance influences LOH. Genetic drift in organisms with rare sex, a space inhabited by numerous protozoa and fungi, is expected to lead to epistasis, which ultimately may lead to maladapted hybrids (Dettman *et al.* 2007) that could rapidly adapt by LOH.

Acknowledgments

We thank Calum Maclean, Emmi Mueller, Jimi Ngyuen, Sujal Phadke, and Serena Zhao for advice and technical support during this project. We thank the P. J. Wittkopp and J. Zhang laboratories for providing strains and for sharing laboratory space. This work was made possible by a grant from the National Institutes of Health, National Institute of Allergy and Infectious Diseases (5R21AI105167-02).

Literature Cited

Anderson, J. B., J. Funt, D. A. Thompson, S. Prabhu, A. Socha *et al.*, 2010 Determinants of divergent adaptation and Dobzhansky-Muller interaction in experimental yeast populations. Curr. Biol. 20: 1383–1388. https://doi.org/10.1016/j.cub.2010.06.022

Auguié, B., 2017 gridExtra: miscellaneous functions for "Grid" graphics, R package version 2.3. https://CRAN.R-project.org/package=gridExtra.

Bailey, S. F., F. Blanquart, T. Bataillon, and R. Kassen, 2017 What drives parallel evolution?: how population size and mutational variation contribute to repeated evolution. BioEssays 39: 1–9. https://doi.org/10.1002/bies.201600176

Basra, P., A. Alsaadi, G. Bernal-Astrain, M. L. O'Sullivan, B. Hazlett *et al.*, 2018 Fitness tradeoffs of antibiotic resistance in extra-intestinal pathogenic *Escherichia coli*. Genome Biol. Evol. 10: 667–679. https://doi.org/10.1093/gbe/evy030

Bennett, R. J., A. Forche, and J. Berman, 2014 Rapid mechanisms for generating genome diversity: whole ploidy shifts, aneuploidy, and loss of heterozygosity. Cold Spring Harb. Perspect. Med. 4: a019604. https://doi.org/10.1101/cshperspect.a019604

Bergström, A., J. T. Simpson, F. Salinas, B. Barre, L. Parts *et al.*, 2014 A high-definition view of functional genetic variation from natural yeast genomes. Mol. Biol. Evol. 31: 872–888. https://doi.org/10.1093/molbev/msu037

Blount, B. A., M. R. M. Driessen, and T. Ellis, 2016 GC preps: fast and easy extraction of stable yeast genomic DNA. Sci. Rep. 6: 26863. https://doi.org/10.1038/srep26863

Boeva, V., T. Popova, K. Bleakley, P. Chiche, J. Cappo *et al.*, 2012 Control-FREEC: a tool for assessing copy number and allelic content using next-generation sequencing data. Bioinformatics 28: 423–425. https://doi.org/10.1093/bioinformatics/btr670

Bolger, A. M., M. Lohse, and B. Usadel, 2014 Trimmomatic: a flexible trimmer for Illumina sequence data. Bioinformatics 30: 2114–2120. https://doi.org/10.1093/bioinformatics/btu170

Burke, M. K., G. Liti, and A. D. Long, 2014 Standing genetic variation drives repeatable experimental evolution in outcrossing populations of *Saccharomyces cerevisiae*. Mol. Biol. Evol. 31: 3228–3239. https://doi.org/10.1093/molbev/msu256

Chin, B. L., M. A. Frizzell, W. E. Timberlake and G. R. Fink, 2012 FASTER MT: isolation of pure populations of a and α ascospores from *Saccharomyces cerevisiae*. G3 (Bethesda) 2: 449–452. https://doi.org/doi: 10.1534/g3.111.001826

Cingolani, P., A. Platts, L. Wang le, M. Coon, T. Nguyen *et al.*, 2012 A program for annotating and predicting the effects of single nucleotide polymorphisms, SnpEff: SNPs in the genome of *Drosophila melanogaster* strain w1118; iso-2; iso-3. Fly (Austin) 6: 80–92. https://doi.org/10.4161/fly.19695

Ciudad, T., M. Hickman, A. Bellido, J. Berman, and G. Larriba, 2016 Phenotypic consequences of a spontaneous loss of heterozygosity in a common laboratory strain of *Candida albicans*. Genetics 203: 1161–1176. https://doi.org/10.1534/genetics.116.189274

Clowers, K. J., J. L. Will, and A. P. Gasch, 2015 A unique ecological niche fosters hybridization of oak-tree and vineyard isolates of *Saccharomyces cerevisiae*. Mol. Ecol. 24: 5886–5898. https://doi.org/10.1111/mec.13439

Conrad, T. M., A. R. Joyce, M. K. Applebee, C. L. Barrett, B. Xie *et al.*, 2009 Whole-genome resequencing of *Escherichia coli* K-12 MG1655 undergoing short-term laboratory evolution in lactate minimal media reveals flexible selection of adaptive mutations. Genome Biol. 10: R118. https://doi.org/10.1186/gb-2009-10-10-r118

Coste, A., V. Turner, F. Ischer, J. Morschhauser, A. Forche *et al.*, 2006 A mutation in Tac1p, a transcription factor regulating *CDR1* and *CDR2*, is coupled with loss of heterozygosity at chromosome 5 to mediate antifungal resistance in *Candida albicans*. Genetics 172: 2139–2156. https://doi.org/10.1534/genetics.105.054767

Cowen, L. E., D. Sanglard, D. Calabrese, C. Sirjusingh, J. B. Anderson *et al.*, 2000 Evolution of drug resistance in experimental populations of *Candida albicans*. J. Bacteriol. 182: 1515–1522. https://doi.org/10.1128/JB.182.6.1515-1522.2000

Daran-Lapujade, P., J. M. Daran, M. A. Luttik, M. J. Almering, J. T. Pronk *et al.*, 2009 An atypical *PMR2* locus is responsible for hypersensitivity to sodium and lithium cations in the laboratory strain *Saccharomyces cerevisiae* CEN.PK113-7D. FEMS Yeast Res. 9: 789–792. https://doi.org/10.1111/j.1567-1364.2009.00530.x

Datta, A., A. Adjiri, L. New, G. F. Crouse, and S. Jinks Robertson, 1996 Mitotic crossovers between diverged sequences are regulated by mismatch repair proteins in *Saccharomyces cerevisiae*. Mol. Cell. Biol. 16: 1085–1093. https://doi.org/10.1128/MCB.16.3.1085

De Coster, W., S. D'Hert, D. T. Schultz, M. Cruts, and C. Van Broeckhoven, 2018 NanoPack: visualizing and processing long-read sequencing data. Bioinformatics 34: 2666–2669. https://doi.org/10.1093/bioinformatics/bty149

Deem, A., A. Keszthelyi, T. Blackgrove, A. Vayl, B. Coffey *et al.*, 2011 Break-induced replication is highly inaccurate. PLoS Biol. 9: e1000594. https://doi.org/10.1371/journal.pbio.1000594

Dettman, J. R., C. Sirjusingh, L. M. Kohn, and J. B. Anderson, 2007 Incipient speciation by divergent adaptation and antagonistic epistasis in yeast. Nature 447: 585–588. https://doi.org/10.1038/nature05856

Doniger, S. W., H. S. Kim, D. Swain, D. Corcuera, M. Williams *et al.*, 2008 A catalog of neutral and deleterious polymorphism in yeast. PLoS Genet. 4: e1000183. https://doi.org/10.1371/journal.pgen.1000183

Duan, S. F., P. J. Han, Q. M. Wang, W. Q. Liu, J. Y. Shi *et al.*, 2018 The origin and adaptive evolution of domesticated populations of yeast from Far East Asia. Nat. Commun. 9: 2690. https://doi.org/10.1038/s41467-018-05106-7

Dutta, A., G. Lin, A. V. Pankajam, P. Chakraborty, N. Bhat *et al.*, 2017 Genome dynamics of hybrid *Saccharomyces cerevisiae* during vegetative and meiotic divisions. G3 (Bethesda) 7: 3669–3679. https://doi.org/doi: 10.1534/g3.117.1135

Ene, I. V., R. A. Farrer, M. P. Hirakawa, K. Agwamba, C. A. Cuomo *et al.*, 2018 Global analysis of mutations driving microevolution of a heterozygous diploid fungal pathogen. Proc. Natl. Acad. Sci. USA 115: E8688–E8697. https://doi.org/10.1073/pnas.1806002115

Fisher, K. J., S. W. Buskirk, R. C. Vignogna, D. A. Marad, and G. I. Lang, 2018 Adaptive genome duplication affects patterns of molecular evolution in *Saccharomyces cerevisiae*. PLoS Genet. 14: e1007396. https://doi.org/10.1371/journal.pgen.1007396

Forche, A., P. T. Magee, A. Selmecki, J. Berman, and G. May, 2009 Evolution in *Candida albicans* populations during a single passage through a mouse host. Genetics 182: 799–811. https://doi.org/10.1534/genetics.109.103325

Forche, A., D. Abbey, T. Pisithkul, M. A. Weinzierl, T. Ringstrom *et al.*, 2011 Stress alters rates and types of loss of heterozygosity in *Candida albicans*. mBio 2: e00129-11. https://doi.org/10.1128/mBio.00129-11

Gerstein, A. C., A. Kuzmin, and S. P. Otto, 2014 Loss-of-heterozygosity facilitates passage through Haldane's sieve for *Saccharomyces cerevisiae* undergoing adaptation. Nat. Commun. 5: 3819. https://doi.org/10.1038/ncomms4819

Gietz, R. D., and R. H. Schiestl, 2007 Quick and easy yeast transformation using the LiAc/SS carrier DNA/PEG method. Nat. Protoc. 2: 35–37. https://doi.org/10.1038/nprot.2007.14

Gimble, F. S., and J. Thorner, 1992 Homing of a DNA endonuclease gene by meiotic gene conversion in *Saccharomyces cerevisiae*. Nature 357: 301–306. https://doi.org/10.1038/357301a0

Goodwin, S. B., B. A. Cohen, and W. E. Fry, 1994 Panglobal distribution of a single clonal lineage of the Irish potato famine fungus. Proc. Natl. Acad. Sci. USA 91: 11591–11595. https://doi.org/10.1073/pnas.91.24.11591

Gorter de Vries, A. R., L. G. F. Couwenberg, M. van den Broek, P. de la Torre Cortés, J. ter Horst *et al.*, 2018 Allele-specific genome editing using CRISPR–Cas9 is associated with loss of heterozygosity in diploid yeast. Nucleic Acids Res. 47: 1362–1372. https://doi.org/10.1093/nar/gky1216

Gresham, D., M. M. Desai, C. M. Tucker, H. T. Jenq, D. A. Pai *et al.*, 2008 The repertoire and dynamics of evolutionary adaptations to controlled nutrient-limited environments in yeast. PLoS Genet. 4: e1000303. https://doi.org/10.1371/journal.pgen.1000303

Hackl, T., R. Hedrich, J. Schultz, and F. Forster, 2014 proovread: large-scale high-accuracy PacBio correction through iterative short read consensus. Bioinformatics 30: 3004–3011. https://doi.org/10.1093/bioinformatics/btu392

Hall, D. W., and S. B. Joseph, 2010 A high frequency of beneficial mutations across multiple fitness components in *Saccharomyces cerevisiae*. Genetics 185: 1397–1409. https://doi.org/10.1534/genetics.110.118307

Hicks, W. M., M. Kim, and J. E. Haber, 2010 Increased mutagenesis and unique mutation signature associated with mitotic gene conversion. Science 329: 82–85. https://doi.org/10.1126/science.1191125

Hill, J. A., T. R. O'Meara, and L. E. Cowen, 2015 Fitness trade-offs associated with the evolution of resistance to antifungal drug combinations. Cell Rep. 10: 809–819. https://doi.org/10.1016/j.celrep.2015.01.009

Hirakawa, M. P., D. A. Martinez, S. Sakthikumar, M. Z. Anderson, A. Berlin *et al.*, 2015 Genetic and phenotypic intra-species variation in *Candida albicans*. Genome Res. 25: 413–425. https://doi.org/10.1101/gr.174623.114

Hope, E. A., and M. J. Dunham, 2014 Ploidy-regulated variation in biofilm-related phenotypes in natural isolates of *Saccharomyces cerevisiae*. G3 (Bethesda) 4: 1773–1786. https://doi.org/doi: 10.1534/g3.114.013250

Hope, E. A., C. J. Amorosi, A. W. Miller, K. Dang, C. S. Heil *et al.*, 2017 Experimental evolution reveals favored adaptive routes to cell aggregation in yeast. Genetics 206: 1153–1167. https://doi.org/10.1534/genetics.116.198895

Hum, Y. F., and S. Jinks-Robertson, 2018 DNA strand-exchange patterns associated with double-strand break-induced and spontaneous mitotic crossovers in *Saccharomyces cerevisiae*. PLoS Genet. 14: e1007302. https://doi.org/10.1371/journal.pgen.1007302

Huxley, C., E. D. Green, and I. Dunham, 1990 Rapid assessment of *S. cerevisiae* mating type by PCR. Trends Genet. 6: 236. https://doi.org/10.1016/0168-9525(90)90190-H

Inbar, E., N. S. Akopyants, M. Charmoy, A. Romano, P. Lawyer *et al.*, 2013 The mating competence of geographically diverse *Leishmania major* strains in their natural and unnatural sand fly vectors. PLoS Genet. 9: e1003672. https://doi.org/10.1371/journal.pgen.1003672

James, T. Y., A. P. Litvintseva, R. Vilgalys, J. A. Morgan, J. W. Taylor *et al.*, 2009 Rapid global expansion of the fungal disease chytridiomycosis into declining and healthy amphibian populations. PLoS Pathog. 5: e1000458. https://doi.org/10.1371/journal.ppat.1000458

Johnson, N. A., 2000 Speciation: Dobzhansky-Muller incompatibilities, dominance and gene interactions. Trends Ecol. Evol. 15: 480–482. https://doi.org/10.1016/S0169-5347(00)01961-3

Koren, S., B. P. Walenz, K. Berlin, J. R. Miller, N. H. Bergman *et al.*, 2017 Canu: scalable and accurate long-read assembly via adaptive k-mer weighting and repeat separation. Genome Res. 27: 722–736. https://doi.org/10.1101/gr.215087.116

Kvitek, D. J., and G. Sherlock, 2011 Reciprocal sign epistasis between frequently experimentally evolved adaptive mutations causes a rugged fitness landscape. PLoS Genet. 7: e1002056. https://doi.org/10.1371/journal.pgen.1002056

Lang, G. I., and A. W. Murray, 2008 Estimating the per-base-pair mutation rate in the yeast *Saccharomyces cerevisiae*. Genetics 178: 67–82. https://doi.org/10.1534/genetics.107.071506

Lang, G. I., D. P. Rice, M. J. Hickman, E. Sodergren, G. M. Weinstock *et al.*, 2013 Pervasive genetic hitchhiking and clonal interference in forty evolving yeast populations. Nature 500: 571–574. https://doi.org/10.1038/nature12344

Laughery, M. F., T. Hunter, A. Brown, J. Hoopes, T. Ostbye *et al.*, 2015 New vectors for simple and streamlined CRISPR-Cas9 genome editing in *Saccharomyces cerevisiae*. Yeast 32: 711–720. https://doi.org/10.1002/yea.3098

Laureau, R., S. Loeillet, F. Salinas, A. Bergström, P. Legoix-Né *et al.*, 2016 Extensive recombination of a yeast diploid hybrid through meiotic reversion. PLoS Genet. 12: e1005781 (erratum: PLoS Genet. 12: e1005953). https://doi.org/10.1371/journal.pgen.1005781

Li, H., 2013 Aligning sequence reads, clone sequences and assembly contigs with BWA-MEM. arXiv 1303: 3997.

Li, H., and R. Durbin, 2009 Fast and accurate short read alignment with Burrows-Wheeler transform. Bioinformatics 25: 1754–1760. https://doi.org/10.1093/bioinformatics/btp324

Liti, G., D. M. Carter, A. M. Moses, J. Warringer, L. Parts *et al.*, 2009 Population genomics of domestic and wild yeasts. Nature 458: 337–341. https://doi.org/10.1038/nature07743

Liu, H. P., C. A. Styles, and G. R. Fink, 1996 *Saccharomyces cerevisiae* S288C has a mutation in *FL08* a gene required for filamentous growth. Genetics 144: 967–978.

MacKenzie, D. A., M. Defernez, W. B. Dunn, M. Brown, L. J. Fuller *et al.*, 2008 Relatedness of medically important strains of *Saccharomyces cerevisiae* as revealed by phylogenetics and metabolomics. Yeast 25: 501–512. https://doi.org/10.1002/yea.1601

Maclean, C. J., B. P. H. Metzger, J.-R. Yang, W.-C. Ho, B. Moyers *et al.*, 2017 Deciphering the genic basis of yeast fitness variation by simultaneous forward and reverse genetics. Mol. Biol. Evol. 34: 2486–2502. https://doi.org/10.1093/molbev/msx151

Magwene, P. M., O. Kayikci, J. A. Granek, J. M. Reininga, Z. Scholl *et al.*, 2011 Outcrossing, mitotic recombination, and life-history trade-offs shape genome evolution in *Saccharomyces cerevisiae*. Proc. Natl. Acad. Sci. USA 108: 1987–1992. https://doi.org/10.1073/pnas.1012544108

Mandegar, M. A., and S. P. Otto, 2007 Mitotic recombination counteracts the benefits of genetic segregation. Proc. Biol. Sci. 274: 1301–1307. https://doi.org/10.1098/rspb.2007.0056

Marad, D. A., S. W. Buskirk, and G. I. Lang, 2018 Altered access to beneficial mutations slows adaptation and biases fixed mutations in diploids. Nat. Ecol. Evol. 2: 882–889. https://doi.org/10.1038/s41559-018-0503-9

McKenna, A., M. Hanna, E. Banks, A. Sivachenko, K. Cibulskis *et al.*, 2010 The genome analysis toolkit: a MapReduce framework for analyzing next-generation DNA sequencing data. Genome Res. 20: 1297–1303. https://doi.org/10.1101/gr.107524.110

McMurray, M. A., and D. E. Gottschling, 2003 An age-induced switch to a hyper-recombinational state. Science 301: 1908–1911. https://doi.org/10.1126/science.1087706

Nieuwenhuis, B. P. S., and T. Y. James, 2016 The frequency of sex in fungi. Philos. Trans. R. Soc. Lond. B Biol. Sci. 371: 20150540. https://doi.org/10.1098/rstb.2015.0540

Novo, M., A. Mangado, M. Quiros, P. Morales, Z. Salvado *et al.*, 2013 Genome-wide study of the adaptation of *Saccharomyces cerevisiae* to the early stages of wine fermentation. PLoS One 8: e74086. https://doi.org/10.1371/journal.pone.0074086

Ogle, D. H., 2018 FSA: fisheries stock analysis, R package version *0.8.20*.
Omilian, A. R., M. E. Cristescu, J. L. Dudycha, and M. Lynch, 2006 Ameiotic recombination in asexual lineages of *Daphnia*. Proc. Natl. Acad. Sci. USA 103: 18638–18643 (corrigenda: Proc. Natl. Acad. Sci. USA 104: 2554). https://doi.org/10.1073/pnas.0606435103
Orr, H. A., 2010 The population genetics of beneficial mutations. Philos. Trans. R. Soc. Lond. B Biol. Sci. 365: 1195–1201. https://doi.org/10.1098/rstb.2009.0282
Parts, L., F. A. Cubillos, J. Warringer, K. Jain, F. Salinas *et al.*, 2011 Revealing the genetic structure of a trait by sequencing a population under selection. Genome Res. 21: 1131–1138. https://doi.org/10.1101/gr.116731.110
Peter, J., M. De Chiara, A. Friedrich, J. X. Yue, D. Pflieger *et al.*, 2018 Genome evolution across 1,011 *Saccharomyces cerevisiae* isolates. Nature 556: 339–344. https://doi.org/10.1038/s41586-018-0030-5
Phadke, S. S., C. J. Maclean, S. Y. Zhao, E. A. Mueller, L. A. Michelotti *et al.*, 2018 Genome-wide screen for *Saccharomyces cerevisiae* genes contributing to opportunistic pathogenicity in an invertebrate model host. G3 (Bethesda) 8: 63–78. https://doi.org/doi: 10.1534/g3.117.300245
Piotrowski, J. S., S. Nagarajan, E. Kroll, A. Stanbery, K. E. Chiotti *et al.*, 2012 Different selective pressures lead to different genomic outcomes as newly-formed hybrid yeasts evolve. BMC Evol. Biol. 12: 46. https://doi.org/10.1186/1471-2148-12-46
R Core Team, 2019 R: A Language and Environment for Statistical Computing. R Foundation for Statistical Computing, Vienna.
Ropars, J., C. Maufrais, D. Diogo, M. Marcet-Houben, A. Perin *et al.*, 2018 Gene flow contributes to diversification of the major fungal pathogen *Candida albicans*. Nat. Commun. 9: 2253. https://doi.org/10.1038/s41467-018-04787-4
Rosen, D. M., E. M. Younkin, S. D. Miller, and A. M. Casper, 2013 Fragile site instability in *Saccharomyces cerevisiae* causes loss of heterozygosity by mitotic crossovers and break-induced replication. PLoS Genet. 9: e1003817. https://doi.org/10.1371/journal.pgen.1003817
Rosenthal, P. J., 2013 The interplay between drug resistance and fitness in malaria parasites. Mol. Microbiol. 89: 1025–1038. https://doi.org/10.1111/mmi.12349
Rossignol, T., L. Dulau, A. Julien, and B. Blondin, 2003 Genome-wide monitoring of wine yeast gene expression during alcoholic fermentation. Yeast 20: 1369–1385. https://doi.org/10.1002/yea.1046
Ruiz, A., and J. Arino, 2007 Function and regulation of the *Saccharomyces cerevisiae ENA* sodium ATPase system. Eukaryot. Cell 6: 2175–2183. https://doi.org/10.1128/EC.00337-07
Ryland, G. L., M. A. Doyle, D. Goode, S. E. Boyle, D. Y. H. Choong *et al.*, 2015 Loss of heterozygosity: what is it good for? BMC Med. Genomics 8: 45. https://doi.org/10.1186/s12920-015-0123-z
Sadhu, M. J., J. S. Bloom, L. Day, and L. Kruglyak, 2016 CRISPR-directed mitotic recombination enables genetic mapping without crosses. Science 352: 1113–1116. https://doi.org/10.1126/science.aaf5124
Schoustra, S. E., A. J. M. Debets, M. Slakhorst, and R. F. Hoekstra, 2007 Mitotic recombination accelerates adaptation in the fungus *Aspergillus nidulans*. PLoS Genet. 3: e68. https://doi.org/10.1371/journal.pgen.0030068
Selmecki, A., A. Forche, and J. Berman, 2006 Aneuploidy and isochromosome formation in drug-resistant *Candida albicans*. Science 313: 367–370. https://doi.org/10.1126/science.1128242
Selmecki, A., A. Forche, and J. Berman, 2010 Genomic plasticity of the human fungal pathogen *Candida albicans*. Eukaryot. Cell 9: 991–1008. https://doi.org/10.1128/EC.00060-10
Sharp, N. P., L. Sandell, C. G. James, and S. P. Otto, 2018 The genome-wide rate and spectrum of spontaneous mutations differ between haploid and diploid yeast. Proc. Natl. Acad. Sci. USA 115: E5046–E5055. https://doi.org/10.1073/pnas.1801040115
Sirr, A., A. C. Scott, G. A. Cromie, C. L. Ludlow, V. Ahyong *et al.*, 2018 Natural variation in *SER1* and *ENA6* underlie condition-specific growth defects in *Saccharomyces cerevisiae*. G3 (Bethesda) 8: 239–251. https://doi.org/doi: 10.1534/g3.117.300392
Smukowski Heil, C. S., C. G. DeSevo, D. A. Pai, C. M. Tucker, M. L. Hoang *et al.*, 2017 Loss of heterozygosity drives adaptation in hybrid yeast. Mol. Biol. Evol. 34: 1596–1612. https://doi.org/10.1093/molbev/msx098
Sniegowski, P. D., P. G. Dombrowski, and E. Fingerman, 2002 *Saccharomyces cerevisiae* and *Saccharomyces paradoxus* coexist in a natural woodland site in North America and display di¡erent levels of reproductive isolation from European conspeci¢cs. FEMS Yeast Res. 1: 299–306.
St Charles, J., E. Hazkani-Covo, Y. Yin, S. L. Andersen, F. S. Dietrich *et al.*, 2012 High-resolution genome-wide analysis of irradiated (UV and γ-rays) diploid yeast cells reveals a high frequency of genomic loss of heterozygosity (LOH) events. Genetics 190: 1267–1284. https://doi.org/10.1534/genetics.111.137927
Steenwyk, J., and A. Rokas, 2017 Extensive copy number variation in fermentation-related genes among *Saccharomyces cerevisiae* wine strains. G3 (Bethesda) 7: 1475–1485. https://doi.org/doi: 10.1534/g3.117.040105
Stovicek, V., C. Holkenbrink, and I. Borodina, 2017 CRISPR/Cas system for yeast genome engineering: advances and applications. FEMS Yeast Res. 17: fox030. https://doi.org/10.1093/femsyr/fox030
Symington, L. S., R. Rothstein, and M. Lisby, 2014 Mechanisms and regulation of mitotic recombination in *Saccharomyces cerevisiae*. Genetics 198: 795–835. https://doi.org/10.1534/genetics.114.166140
Treangen, T. J., B. D. Ondov, S. Koren, and A. M. Phillippy, 2014 The Harvest suite for rapid core-genome alignment and visualization of thousands of intraspecific microbial genomes. Genome Biol. 15: 524. https://doi.org/10.1186/s13059-014-0524-x
Vázquez-Garcia, I., F. Salinas, J. Li, A. Fischer, B. Barré *et al.*, 2017 Clonal heterogeneity influences the fate of new adaptive mutations. Cell Rep. 21: 732–744. https://doi.org/10.1016/j.celrep.2017.09.046
Wang, Q. M., W. Q. Liu, G. Liti, S. A. Wang, and F. Y. Bai, 2012 Surprisingly diverged populations of *Saccharomyces cerevisiae* in natural environments remote from human activity. Mol. Ecol. 21: 5404–5417. https://doi.org/10.1111/j.1365-294X.2012.05732.x
Warringer, J., and A. Blomberg, 2003 Automated screening in environmental arrays allows analysis of quantitative phenotypic profiles in *Saccharomyces cerevisiae*. Yeast 20: 53–67. https://doi.org/10.1002/yea.931
Warringer, J., E. Zorgo, F. A. Cubillos, A. Zia, A. Gjuvsland *et al.*, 2011 Trait variation in yeast is defined by population history. PLoS Genet. 7: e1002111. https://doi.org/10.1371/journal.pgen.1002111
Wertheimer, N. B., N. Stone, and J. Berman, 2016 Ploidy dynamics and evolvability in fungi. Philos. Trans. R. Soc. Lond. B Biol. Sci. 371: 20150461. https://doi.org/10.1098/rstb.2015.0461
Wickham, H., 2009 *ggplot2: Elegant Graphics for Data Analysis*. Springer-Verlag, New York.
Wiser, M. J., and R. E. Lenski, 2015 A comparison of methods to measure fitness in *Escherichia coli*. PLoS One 10: e0126210. https://doi.org/10.1371/journal.pone.0126210
Wu, C. I., and C. T. Ting, 2004 Genes and speciation. Nat. Rev. Genet. 5: 114–122. https://doi.org/10.1038/nrg1269

Zerbino, D. R., and E. Birney, 2008 Velvet: algorithms for de novo short read assembly using de Bruijn graphs. Genome Res. 18: 821–829. https://doi.org/10.1101/gr.074492.107

Zeyl, C., T. Vanderford, and M. Carter, 2003 An evolutionary advantage of haploidy in large yeast populations. Science 299: 555–558. https://doi.org/10.1126/science.1078417

Zhang, K., D. Q. Zheng, Y. Sui, L. Qi, and T. D. Petes, 2019 Genome-wide analysis of genomic alterations induced by oxidative DNA damage in yeast. Nucleic Acids Res. 47: 3521–3535. https://doi.org/10.1093/nar/gkz1027

Zhu, Y. O., M. L. Siegal, D. W. Hall, and D. A. Petrov, 2014 Precise estimates of mutation rate and spectrum in yeast. Proc. Natl. Acad. Sci. USA 111: E2310–E2318. https://doi.org/10.1073/pnas.1323011111

Communicating editor: A. Mitchell